1809799

by Thomas Grennan

Submission date: 21-Jan-2022 11:02PM (UTC+0000)
Submission ID: 169969889
File name: 11301_Thomas_Grennan_1809799_179509_476361696.pdf (7.31M)
Word count: 12034
Character count: 74020

Course: BSc (Hons) Electrical and Electronic Engineering

Module: SGEE6001 – Power Electronics and Drives

Assignment: Investigation into DC drives and control methods

Name: Thomas Grennan

University number: 1809799

Date submitted: 21/01/2022

Word count: 4437

Word count exceeded

Good summary but it is too long

Excellent evidence of research, all relevant but again too long and too much detail

Your assessment of business and customer needs is particularly good

Simulation, design adaptation and practical work are excellent with support for results from research

Good conclusions and recommendation presented

However, report is too long

Contents

Table of Figures 3

Table of Tables 4

Executive Summary 5

1. Research 6

1.1 Design features and control techniques employed in a three-phase, four quadrant DC drive currently available from one DC drive manufacturer 6

1.2 Typical applications of four quadrant DC drives, making comparisons with other DC drives including single-phase converters and chopper drives, and with modern AC drives 10

1.3 Selection of motor drives for industrial applications based on business, customer and user needs including the wider engineering context, aesthetics, operation, maintenance and reliability 13

2. Simulation and Design Adaption 15

2.1 Three-Phase Full Wave Fully Controlled Rectifier 15

2.2 Design Adaptation 17

3. Practical Investigations 20

3.1 Experimental Setup 20

3.2 Four Quadrant Operation 21

3.3 DC Motor Analysis – 3 different speed set-points 24

3.3.1 Motor Constants 25

3.4 DC Motor Analysis – 3 different torque set-points 27

3.5 Analysis of the DCMs Performance 28

4. Overall Conclusions and Recommendations 29

5. Team Working and Health & Safety Precautions 32

6. Works Cited 33

7. Appendix 36

7.1 Appendix for Section 1 36

7.1.1 Sinamics Application Class 36

7.1.2 Siemens Sinamics DCM control circuit 37

7.1.3 – Industrial hoist system explanation 38

7.2 Appendix for Section 2 39

7.2.1 Simulation Thyristor Data Sheet 39

7.2.2 – Simulation Calculations and Waveforms 40

7.2.3 – Design and Adaptation for Three-phase fully-controlled dual bridge converter 46

7.2.4 Krishnans Theory of Four quadrant operation 47

7.2.5 – Testing for Three-phase fully-controlled dual bridge converter 48

7.3 Appendix for Section 3 50

7.3.1 Explanation of experimental set-up, drive connections and measuring equipment 50

7.3.2 Demonstration of Four Quadrant Operation 58

7.3.3 3 values of speed at a constant torque 62
7.3.4 3 values of torque at a constant speed 68

Table of Figures

Figure 1 – Sinamics 6RA8013-6DV62-0AA0 Power Circuit (Siemens, 2012) 6
Figure 2 – Speed and Current Closed Loop Control (Siemens, 2012) 8
Figure 3 – Close-loop control structure (Siemens, 2014) 9
Figure 4 – Sinamics DCM retrofitted to a Ward-Leonard block (Siemens, 2013) 11
Figure 5 – Multisim model of Three-Phase Full Wave Fully Controlled Rectifier 15
Figure 6 – Three-phase fully-controlled dual rectifier (Rashid, 2018) 17
Figure 7 – Four-quadrant simulation results 18
Figure 8 – Experimental set-up 20
Figure 9 – HMI: Practical Four Quadrant Operation 21
Figure 10 - Picoscope: Practical Four Quadrant Operation 21
Figure 11 – Picoscope graph with cursors for motor constants 25
Figure 12 – Motor constants: HMI Values 26
Figure 13 – Sinamics DCM Application Class 1 (Siemens, 2015) 36
Figure 14 – Sinamics DCM Application Class 2 (Siemens, 2015) 36
Figure 15 – Sinamics DCM Control Circuit (Siemens, 2012) 37
Figure 16 – Four quadrant operation for hoisting (eeeguide, 2016) 38
Figure 17 – Datasheet for BTW42-600R SCR 39
Figure 18 – Simulation Testing: Firing Angle set to 0° 40
Figure 19 - Simulation Testing: Vmax found at 575.466V 40
Figure 20 - Simulation Test 1: 10° Degree Firing Angle 41
Figure 21 - $VMAX$ found at 575.466V 41
Figure 22 - Simulation Test 2: 20° Degree Firing Angle 42
Figure 23 - Simulation Test 2: Armature Voltage & Current at 20° 43
Figure 24 - Simulation Test 3: 30° Degree Firing Angle 44
Figure 25 - Simulation Test 3: Armature Voltage & Current at 30° 44
Figure 26 – Main Circuit: Three-phase fully-controlled dual bridge converter adaptation 46
Figure 27 - Auxiliary Circuit: Three-phase fully-controlled dual bridge converter adaptation 46
Figure 28 – Krishnans theory of four quadrant operation (Krishnan, 2001) 47
Figure 29 - Simulation Adaptation: Quadrant 1 48
Figure 30 - Simulation Adaptation: Quadrant 2 48
Figure 31 - Simulation Adaptation: Quadrant 3 49
Figure 32 - Simulation Adaptation: Quadrant 4 49
Figure 33 – Practical Control Panel Schematics: Mains Supply 52
Figure 34 Practical Control Panel Schematics: S120, DCM & DC Motor (Inc. Picoscope & Power Analyser) 53
Figure 35 - Practical Control Panel Schematics: 24V Distribution, HMI and Ethernet Switch 54
Figure 36 – Practical Control Panel Schematics: Siemens S7-1500 PLC 55
Figure 37 – Practical Control Panel Schematics: Safety Inputs 56
Figure 38 - Practical Control Panel Schematics: Safety Outputs 57
Figure 39 – Practical: Quadrant 1 operation (Picoscope) 58
Figure 40 - Practical: Quadrant 1 operation (HMI) 58
Figure 41 Practical: Quadrant 2 operation (Picoscope) 59
Figure 42 Practical: Quadrant 2 operation (HMI) 59
Figure 43 - Practical: Quadrant 3 operation (Picoscope) 60
Figure 44 - Practical: Quadrant 3 operation (HMI) 60

Figure 45 - Practical: Quadrant 4 operation (Picoscope) 61
Figure 46 - Practical: Quadrant 4 operation (HMI) 61
Figure 47 – Practical Speed test: Setpoint 1 Picoscope 62
Figure 48 - Practical Speed test: Setpoint 1 HMI 62
Figure 49 - Speed test: Setpoint 1 Power Analyser 63
Figure 50 - Practical Speed test: Setpoint 2 Picoscope 63
Figure 51 - Practical Speed test: Setpoint 2 HMI 64
Figure 52 - Practical Speed test: Setpoint 2 Power Analyser 64
Figure 53 - Practical Speed test: Setpoint 3 Picoscope 65
Figure 54 - Practical Speed test: Setpoint 3 HMI 65
Figure 55 - Practical Speed test: Setpoint 3 Power Analyser 66
Figure 56 - Practical Torque test: Setpoint 1 Picoscope 68
Figure 57 - Practical Torque test: Setpoint 1 HMI 68
Figure 58 - Practical Torque test: Setpoint 1 Power Analyser 69
Figure 59 - Practical Torque test: Setpoint 2 Picoscope 69
Figure 60 - Practical Torque test: Setpoint 2 HMI 70
Figure 61 -Practical Torque test: Setpoint 2 Power Analyser 70
Figure 62 - Practical Torque test: Setpoint 3 Picoscope 71
Figure 63 - Practical Torque test: Setpoint 3 HMI 71
Figure 64 - Practical Torque test: Setpoint 3 Power Analyser 72

Table of Tables

Table 1 - Fully-Controlled Three Phase Rectifier Test - 3 Firing Angles 17
Table 2 - Four Quadrant Operation: Comparison between Theory and Simulation 19
Table 3: Four Quadrant Operation: Comparison between Theory and Practical 22
Table 4 - Four Quadrant Operation: Comparison of Motor Parameters in 4 Quadrants 22
Table 5 - DCM Performance : 3 Speeds at a Constant Load Torque 24
Table 6 - DCM Performance: 3 Torque values at a constant speed 27

Executive Summary

This report is focused on DC drives and control methods, specifically the Sinamics DCM and its performance. Research undertaken into the design features and control techniques of the DCM found that it is implemented with two thyristor bridges in anti-parallel in a circulating-current free configuration. From a control aspect it is found that the functionality is exceptional, implementing fieldbus communications for ease of use, along with multiple control-loops for various applications. Further research found that the DCMs are utilised in retrofitting applications such as Ward-Leonard blocks where the motor-generator block is still operational but requires upgrading for safety or new requirements, other applications include hoisting systems. However, it was found that AC motors and DC motors with chopper drives perform some applications just as well. The selection of motor drives was also researched, it was found that there are many factors that determine the selection, including cost, functionality, risk assessments, performance level and end-user requirements.

Simulations were undertaken on a separately-excited DC motor model controlled by a fully-controlled three-phase rectifier. Suitable test equipment was implemented in the circuit allowing for analysis of the armature voltage under three different firing angles, from this it was found that the firing angle has a direct effect on the armature voltage, the greater the firing angle the smaller the armature voltage. The simulation was then adapted, an extra bridge of thyristors connected in anti-parallel enables operation in all four quadrants, testing was undertaken and compared with theory proving the adaptations credibility.

Practical experiments were undertaken on a DC motor controlled by a Sinamics DCM drive, four-quadrant operation was tested on the drive, suitable measuring equipment provided values to be compared and contrasted to the drive, the values obtained correlated with theory and simulation proving the reliability of the system. Two further tests were undertaken, these analysed the effects that varying speed and torque had on the motors characteristics. From these tests, the relationship between speed & voltage and torque & current is evident, ultimately proving the theories of various engineers and authors, along with the previous simulations. The DCMs performance was analysed, the performance was found successful as it provided results that were highly comparable to simulation and theory.

The conclusion demonstrated the success of the report, outlining how firm comparisons were made between theory, simulation and practical. It was found that all information obtained was relevant and comparable between one another, whilst outlining the usefulness of the test equipment and theoretical calculations used to add extra grounds for comparison. Recommendations were made to provide testing of AC induction motors and chopper drives in four quadrants to practically compare the performance against the separately-excited DC motor.

1. Research

1.1 Design features and control techniques employed in a three-phase, four quadrant DC drive currently available from one DC drive manufacturer

The Sinamics DC Master from Siemens (6RA8013-6DV62-0AA0) is designed to supply the field and armature of variable-speed DC motors, along with other applications including the field control of synchronous generators. The Sinamics DCM unit are compact units, consisting of both power units for the armature and field supply, as well as control circuits and options for additional modules for communications, enabling the commissioning of the system to be fully tailored to the application. The DCM is offered in units rated from 15Adc to 1200Adc. All DCM models are equipped with a Basic Operator Panel as standard, allowing for parameters to be read and edited during commissioning, whilst displaying measured values, alarms and fault codes (Siemens, 2012).

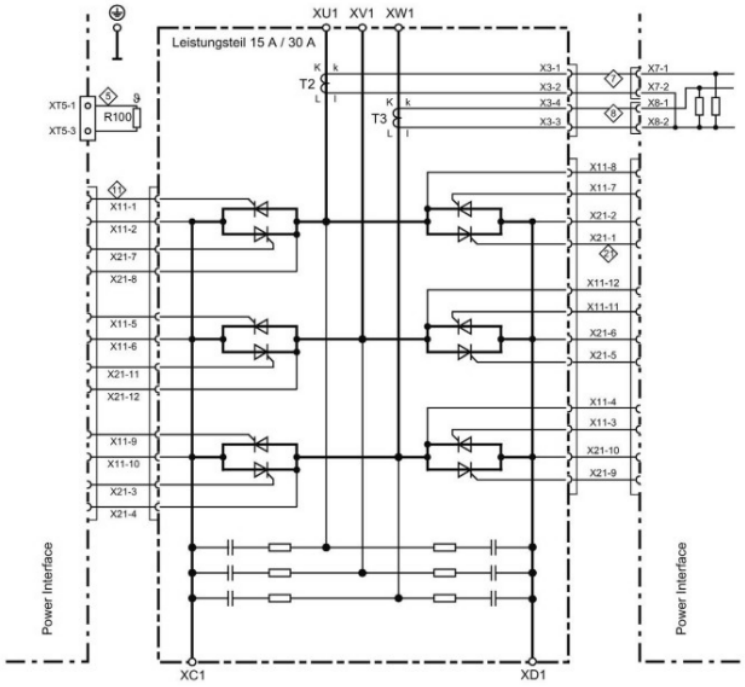


Figure 1 – Sinamics 6RA8013-6DV62-0AA0 Power Circuit (Siemens, 2012)

The armature and field power units consist of electrically insulated thyristor modules, with the four-quadrant unit models supplying the armature via two fully-controlled three-phase bridges. Bridge 1 supplies positive current to the motor, whilst bridge 2 supplies negative current. Many four-quadrant drives are designed so that the voltages are coequal ensuring that circulating currents caused by

potential difference between bridges are minimal, however, this is fictitious to assume in real world applications where potential difference occurs between converters, creating circulating currents. Circulating currents can be minimised by connecting a reactor between bridges to smooth and limit ripple currents by allowing both bridges to conduct equally (Drury, 2013). The Sinamics DCM removes the need for a reactor between bridges, bridge 1 and 2 are connected in an anti-parallel circulating current free configuration, this ensures that both converters are unable to operate simultaneously (Siemens, 2015). The changeover from converter 1 to converter 2 is only possible when the firing pulses are removed and the armature current decays to 0A, this is enabled in the DCM through a zero-current detection circuit which provides a torque-free timeframe of 10ms to safely change between converters (Drury, 2013).

Figure 1 displays the 6RA8013-6DV62-0AA0 power circuit, this shows the 6 pairs of thyristors utilised in dual three-phase fully controlled converters, showing the connecting terminals for the SCRs gate. The power circuit shows an RC snubber circuit connected in parallel with the thyristors, this limits the rate at which the anode voltage spikes during its turn-off period in-turn improving the performance of the switching circuit by supressing the effects of $^{dv}/_{dt}$ and reducing electromagnetic interference (Lander, 1993).

The Sinamics DCM is implemented with the *'CUD'* control unit, allowing for engineers to commission a system tailored to the end-users needs. Within the control unit various I/O functionalities are available including digital and analog I/O, pulse encoder terminals, bidirectional I/O, motor thermistors, fieldbus communications including RS-485 for additional operator panels and USS interfaces and DRIVE-CLiQ interface for interface with Sinamics drive system with various manufacturers whilst offering integrated safety functions (Siemens, 2013).

The DCM offers communications through various different protocols including PROFIdrive, PROFINET I/O, SINAMICS Link, EtherNet/IP and PROFIBUS. PROFIdrive is the standard profile for drive technology in concurrence with PROFIBUS & PROFINET allowing for I/O mapping to both sub-protocols. PROFIdrive uses open application profiles divided into classes to enable controllers such as PLCs and DCS systems to connect to drives for control and parameterisation applications. PROFIdrive eliminates the need for external-device monitoring through force-guided relays providing feedback. PROFIdrive is implemented with PROFIsafe, both profiles create a harmonious unit enabling a bus sharing system between the drives standard functions and safety functions, enabling motion control and safety control of the DCM simultaneously (PROFIBUS, 2019).

Application Class 1 is the most basic method of control, this is the standard drive application. The drive is controlled by a speed set-point through PROFINET/PROFIBUS for both open and closed loop control, in this application class the speed control is handled completely by the drive controller (profibus, 2020).

Application Class 2 is the standard drive function with technology, where the drive communicates with a PLC via PROFINET/PROFIBUS. In this application the total process is divided into small sub-processes distributed among multiple drives, therefore the automation functions no longer reside in the PLC but also in the drive controller. This application is used for set-point cascades, winding drives and speed synchronization. Block diagrams for both application class 1 & 2 are seen in figures 13 & 14 in appendix 7.1.1 (profibus, 2020).

The DCM implements a Proportional-Integral controller for speed control, this controller corrects the error between the speed set-point and the actual motor speed based on feedback. The DCM offers additional properties to the PI controller such as a *'Lead/lag element'* which improves the speed control stability in speed critical applications, this function allows for connection to the actual speed value channel. For applications with large loads the *'start pulse'* property can be used, the '*I*' part is started with a selectable value in order to prevent the load from sagging. *'Droop'* is a function used to feedback the 'I' component to the input, this function does not control the set-point but allows a continuous set-point actual deviation, this is required in applications where two drives are mechanically coupled in production machines, *'droop'* prevents both drives operating against one another (Siemens, 2018).

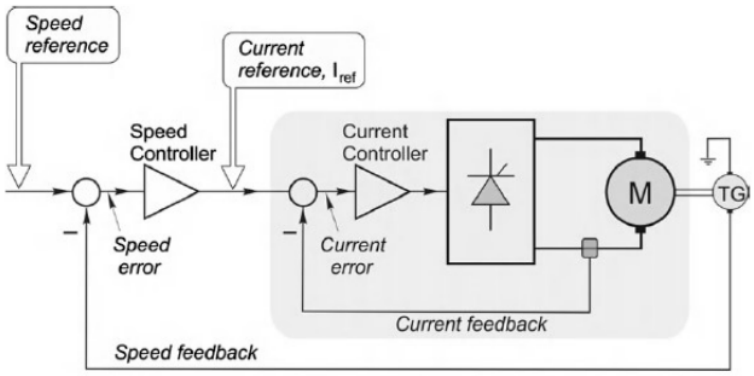


Figure 2 – Speed and Current Closed Loop Control (Siemens, 2012)

The DCM also provides control techniques for auto-reversal, the auto reversal module ensures that a logical sequence occurs for all processes and operations required when reversing the torque direction. A current controller is implemented as a PI controller with P gain and independently set integral time, P & I can be individually turned off to turn the controller into a pure P or pure I controller, the actual current is sensed by a current transformer seen on the three-phase supply. This is fed into the controller via load resistor and rectifier after the analog-to-digital conversion at 10bits for the DCMs rated current, the current controller output transfers the firing angle to the gating unit. The gating unit generates firing pulses for the power thyristors in synchronicity with the line voltage, the timing of these pulses is dependent the control values and output values of the current controller. These control functions are shown in the closed-loop control structure in figure 3 (Siemens, 2014).

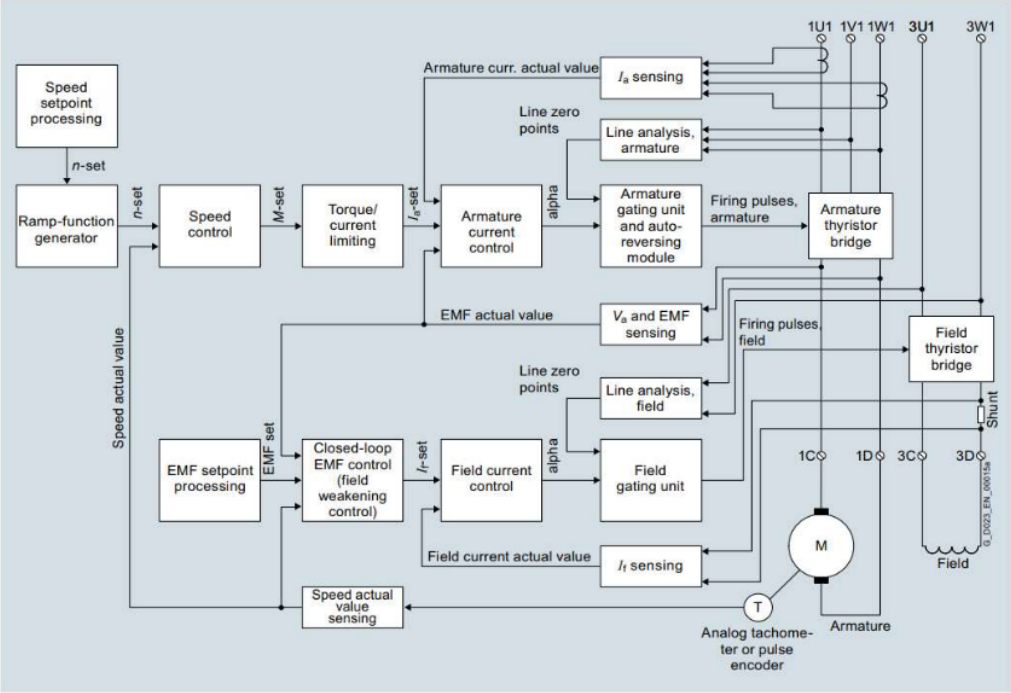


Figure 3 – Close-loop control structure (Siemens, 2014)

1.2 Typical applications of four quadrant DC drives, making comparisons with other DC drives including single-phase converters and chopper drives, and with modern AC drives

Four-quadrant DC drives are used in a wide range of industries such as mining and metals in steelworks, plastic extrusion, paper manufacturing, oil and gas. In applications such as rolling mills, wire drawing machines, presses, elevators and cranes, hoists and cableways. DC Drives such as the Sinamics DCM offer a large scale of applications where their system can be used in open and closed-loop speed and torque control in motors from 6kW to 30MW (Siemens, 2018).

One of the main applications where four-quadrant DC drives such as the Sinamics DCM are used are in retrofitting applications in existing plants and systems such as rolling steel mills and hoists. Within many manufacturing plants there are numerous DC installations which cannot be controlled by modern automation systems such as AC drives. The ability of implementing the DCM into existing systems allows the mechanical system, motor and power wiring to be preserved whilst the closed-loop control system is replaced by the DCM control module, allowing older systems to compete with new systems by only changing the drive and simple parameterisation (Siemens, 2014).

An application where the DCM is retrofitted is in Ward-Leonard blocks where the motor-generator block still provides sufficient performance, a low-cost application to modernise the control is implemented with four-quadrant DC drives. The Ward-Leonard block was used for the variable speed control in DC motors, providing four-quadrant control with its ability to buffer a transient load from a supply whilst producing no harmonics made this the preferred drive for four-quadrant operation (Lander, 1993). This system consists of a DC motor supplied by a DC generator driven by synchronous motor. The DC motors armature voltage is controlled by changing the generators armature voltage by changing the field allowing for variable armature voltage control. The generators armature voltage is controlled using a field supply of low power enabling variable speed control of the motor.

Four-quadrant DCM drives are often integrated into older systems for full control of the motor-generator block using standard functions within the drive. Enabling 3 closed-loop functions for full control. Control-loop 1 controls the generator field using the DC drives armature current controller, control-loop 2 controls the generators armature current and control-loop 3 controls the motor speed using the DC drives speed-control function. Four-quadrant control is a requirement for this application to obtain both polarities of generator voltage, enabling motor operation in both rotational directions. When field weakening is a requirement, an extra two-quadrant drive is used to control the motors field (Siemens, 2013).

Figure 4 shows the circuit diagram for this system.

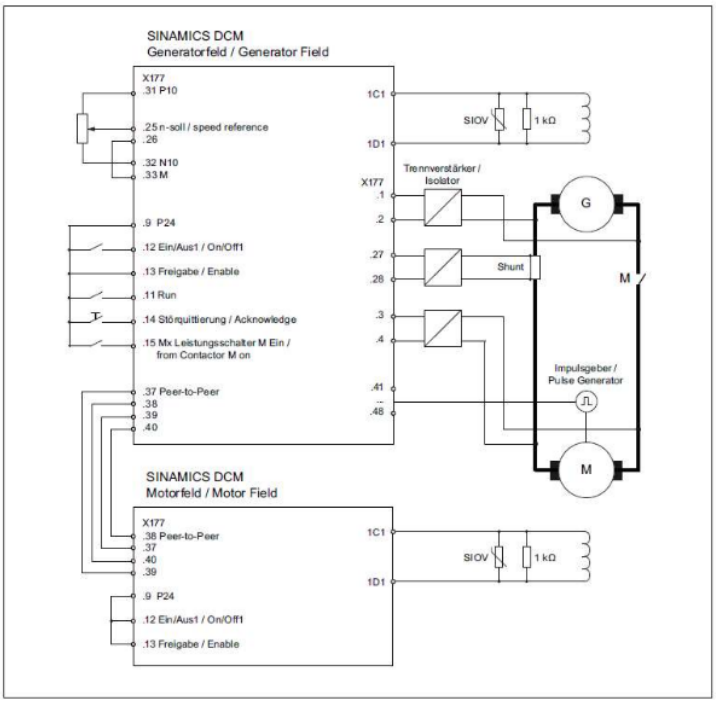


Figure 4 – Sinamics DCM retrofitted to a Ward-Leonard block (Siemens, 2013)

Four-quadrant DC drives are used widely in traction motion control applications, with the most common being industrial hoists due to the requirement of smooth acceleration, fast dynamic response and high efficiency. With the regenerative braking function being used to return energy back to the supply, this is highly effective in frequent transport systems like hoists. The DC motor is the ideal machine for this application due to the frequent starting and braking with large torque loads (Rashid, 2014).

Due to the different scenarios where the hoist may be hoisting upwards or downwards, fully-loaded or load-free four-quadrant control is essential, an explanation of this application is seen in appendix 7.1.3. Using four-quadrant drives for this application removes the requirement for mechanical brakes to stop motion, simplifying the control system.

In previous years DC motors were preferred for certain applications due to their ease of speed control by varying the voltage, whereas AC motors require varying of frequency which was more difficult. In recent years power electronics technology has vastly improved to a point where DC motors are being phased out in favour of AC motors. Modern electronics such as variable frequency drives makes it easy to provide an AC supply with variable frequency making it more economical and efficient to have variable speed using AC motors.

Many manufacturers offer VFDs that allow four-quadrant operation with induction motors such as Omron's MX2 VFD (Omron, 2013). Chopper drives are also used in applications where four-quadrant DC drives have been used. Stepper motors and chopper drives are widely used in traction applications, such as hoisting application seen previously. Modifications allow chopper drives the ability to operate in all four-quadrants, with the ability of regenerative braking it makes this system desirable in transportation applications with frequent stops such as mass rapid transit systems e.g., heavy rail & subways, four-quadrant operation is easily available by reversing the polarity of armature or field voltages and current (Rashid, 2014). The DC chopper is a popular method of DC motor control due to it permitting continuous smooth control of torque and speed whilst using less power compared to a DCM. Chopper drives are also used in autonomous power supply systems for batteries and renewable DC sources such as wind turbines and photovoltaic cells (Wildi, 2014). AC motors are often favoured over DC motors as they are considered more powerful, widely available, more reliable and require less maintenance.

1.3 Selection of motor drives for industrial applications based on business, customer and user needs including the wider engineering context, aesthetics, operation, maintenance and reliability

Motor drive selection is an important aspect that end-users face, selecting the correct drive optimises motor control and manufacturing processes. There are many factors that need to be considered when choosing a drive. There are four areas of opportunity for end-users to improve their manufacturing operations. Opportunity 1 is the boosting of productivity, by selecting the correct drive for an application process, consistency and speeds are increased, reduction of waste and producing higher outputs from optimised motor control. Maximising availability is opportunity 2, downtime reduces profits therefore equipment solely chosen due to low costs may end up costing the end user more in the long term, malfunctioning control equipment halts production and causes revenue losses, choosing the ideal drive for the process ensures that the drive is suited and sized right to the application, in turn performing correctly under no stresses reducing downtime. Opportunity 3 is the reduction of operating costs, reducing operation costs is one of the biggest business requirements. Selecting and implementing the correct drive allows for motor control optimisation consistently with process needs. Optimisation improves energy and running costs as well as reducing raw material waste. Reduction of maintenance costs is opportunity 4. When unexpected downtime occurs a profitable operation can be ruined, choosing a drive company who offers servicing and proactive maintenance can save the customer from hidden costs from downtime which could have been controlled (ABB, 2020).

From a systems integrators and customers point of view, the ease of integration into other control systems is an important aspect when choosing a drive, ensuring that it provides the necessary functionalities including fieldbus communications, functional safety, I/O and parameterization. From a business and customer point-of-view the safety aspect of the drive is integral, to ensure that the drive meets the relevant standards many end-users require drives with integrated fieldbus communications such as PROFIdrive and ‘Failsafe over EtherCAT (FSoE)’ where higher level safe functionalities such as ‘safe speed limit’ are available through the integration with safety PLCs. Therefore, the choice of a motor drive is heavily influenced by the Performance Level of the application as defined by EN ISO 13849-1 as determined by the risk assessment (Lawson, 2019).

Other factors in the wider engineering context such as aesthetics, operation, maintenance and reliability will also influence the choice of drive. Maintenance and engineering personnel are heavily influenced by the operation and reliability of the drive, they are also inclined to choose drives of the same manufacturer as they currently have in their plant, this limits the need for multiple licenses and engineers will have knowledge of the user interface, in turn reducing downtime. Aesthetics of the drive are not essentially relevant, as long as it is designed to manufacturer standards with enough airflow

clearance whilst complying with safety and EMC standards, whilst also offering simple user interfaces. Another aspect often missed is the end user's infrastructure, from an EMC point of view these customers utilities are essential as if the customer has its own supply transformer on site a class A filter can be used, if the supply is straight off the grid class B must be used (Schneider, 2018).

For more specialist applications, the level of technical support available will also influence the type of drive chosen, where suppliers and integrators are able to provide in-depth support creates a selling point for end users (Siemens, 2021).

2. Simulation and Design Adaption

2.1 Three-Phase Full Wave Fully Controlled Rectifier

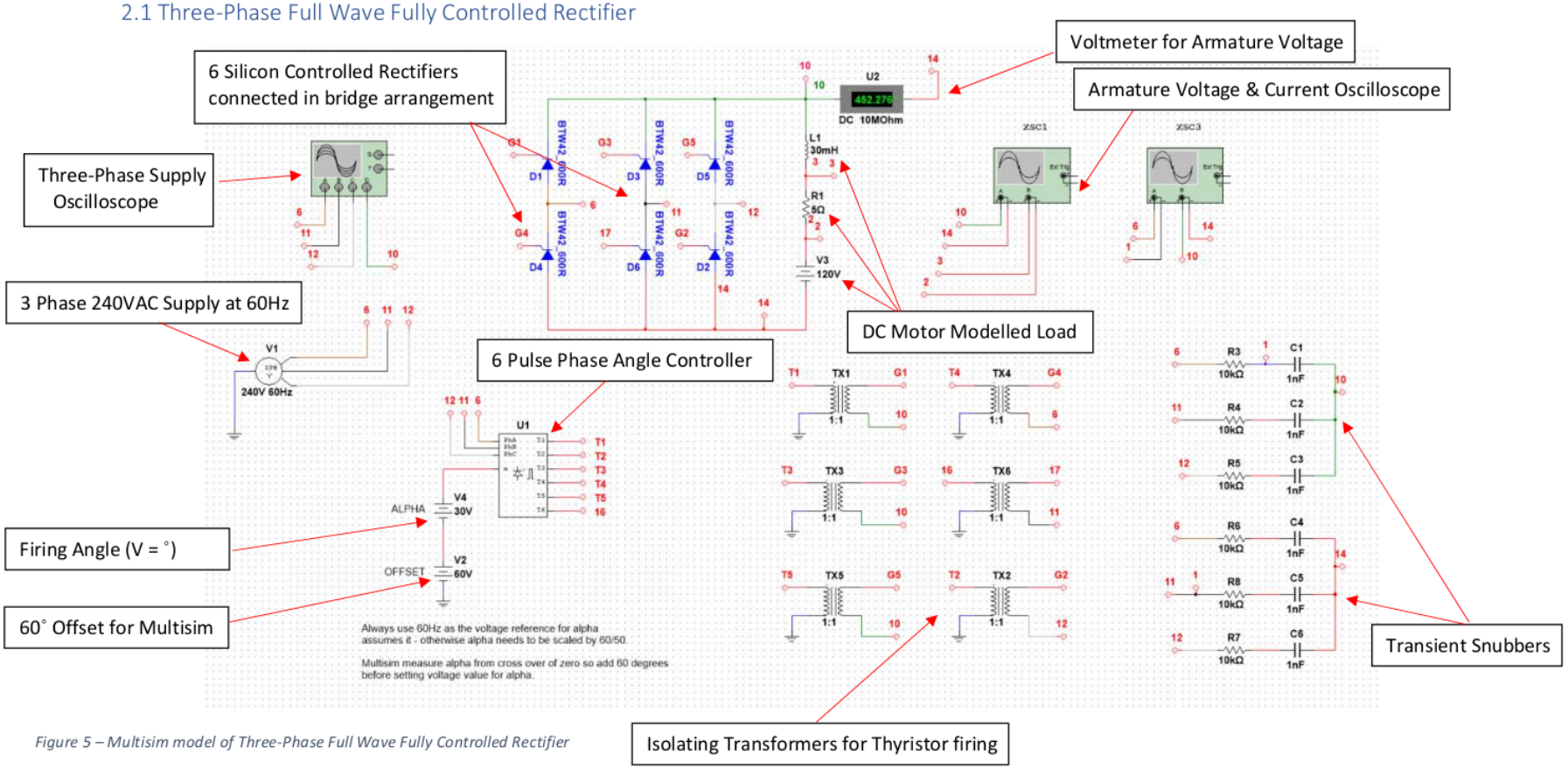


Figure 5 – Multisim model of Three-Phase Full Wave Fully Controlled Rectifier

Figure 5 shows a modelled separately excited motor, the motor is modelled as a load containing an inductor (L), resistor (R) and back EMF (E). Using NI Multisim, the model is simulated. The load is controlled by a fully-controlled three-phase rectifier, a 6-pulse-phase angle controller controls the firing pulses to 6 isolating transformers which isolates the incoming supply from the separated extra-low voltage (SELV) to trigger the SCR gate. 6 Silicon Controlled Rectifiers (SCR) are connected in a bridge arrangement, with three pairs of series SCRs all connected to a common point across the load. Oscilloscopes are connected to measure various waveforms including line voltage, armature voltage and armature current.

A voltage-source in the form of a battery is connected to the phase angle controller to set the firing angle where voltage is directly proportional to firing angle i.e., 30V = 30˚. An offset of 60˚ is connected to the alpha (∝) terminal of the phase-angle controller due to Multisims measuring method.

The SCRs semi-conductor crystal structures are sensitive to electrical stresses. Resistor-Capacitor networks known as '*Snubbers*' are connected in parallel with the SCR, these limit the transient voltage surges as a result of $^{\mathrm{dv}}/_{\mathrm{dt}}$. The SCRs in the design are chosen to be able to deal with the electrical characteristics of the system, the SCRs (BTW42-600R) have a reverse-breakdown-voltage-of-600V (appendix 7.2.1), the simulated circuit has a peak voltage of 339.4V, as seen below.

$$Peak\ Voltage\ = 240V \times \sqrt{2}\ = 339.4$$

The firing angle is set to 0˚, this allows for V_{max} to be determined. Figure 19 in appendix 7.2.2 displays the Multisim cursor displaying V_{max}. The mean armature voltage is calculated using the equation below, where alpha represents the firing angle.

$$V_{mean} = \frac{3 \times V_{max}}{\pi} \times Cos(\propto)$$

The maximum armature voltage is found at 575.466V seen in appendix 7.2.2. Three firing angles were chosen at 10˚, 20˚ and 30˚, all displaying continuous current. Calculations and simulation results are seen in appendix 7.2.2, and table 1 displays a comparison of the results obtained.

Fully-Controlled Three Phase Rectifier Test - 3 Firing Angles			
Firing Angle	Simulation Armature Voltage	Calculated Armature Voltage	Error
10˚	540.478	541.18	0.702
20˚	516.129	516.388	0.259
30˚	475.598	475.907	0.309

Table 1 - Fully-Controlled Three Phase Rectifier Test - 3 Firing Angles

The results in table 1 have proven successful. The chosen firing-angles tests are highly accurate when compared between simulation and calculation proving the reliability of both, with the largest error being 0.702V at 10˚. This is likely due to mathematical rounding of the calculations and the voltage drop across the thyristors which the simulation takes into account.

Both calculation and simulation proved the relationship between firing angle and voltage, that as the firing angle is increased, the armature voltage decreases due to a larger section of the input waveform being removed due to the increased delay.

2.2 Design Adaptation

The full-wave, fully controlled three-phase rectifier seen in section 2.1 is modified to allow for four-quadrant operation. Four-quadrant operation is available in three-phase fully-controlled dual rectifiers seen in figure 6, a second SCR bridge is connected in anti-parallel across the opposite side of the load to provide negative current. Instantaneous voltage differences are present between bridges in dual-converters causing *'Circulating Currents'*. Figure 6 shows circulating-reactors (L_D) connected between the bridge output and the load to limit circulating currents (Rashid, 2018), .

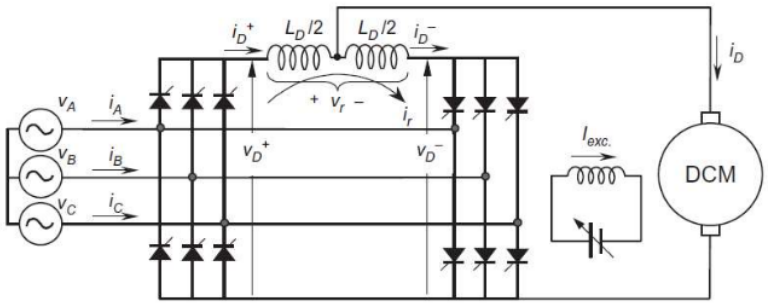


Figure 6 – Three-phase fully-controlled dual rectifier (Rashid, 2018)

Figures 26 & 27 in appendix 7.2,3 shows the circuit adaptation to implement the dual-bridge rectifier. A second SCR bridge is connected in anti-parallel across the opposite side of the load. This design has been modelled on Krishnan & Ramaswamis paper whereby a single firing unit is used, with the pulses

being diverted to the appropriate converter by a master-controller implementing inhibiting signals. This is a ‘circulating-free converter’ which implements a deadtime for a few milliseconds, the converter not supplying current remains blocked, when reversal is required the logic system determines speed and when the conducting converters zero-crossing current falls to zero and the gate-pulses are removed, then allows the opposite converter to conduct, removing needs for circulating-reactors (Ramaswami, 1976).

The first converter was duplicated and connected in anti-parallel across the opposite load side. Multisims parts database does not offer a master-controller, therefore, single-pole single-throw (SPST) switches are connected between the two converters to prevent circulating currents. Four SPST switches are connected in pairs on either side of the back EMF battery to enable four-quadrant operation by reversing the back EMF simulating regenerative braking.

Single-pole-double-throw (SPDT) switches are used on the transformer secondary to switch between which bridge of thyristors are being triggered, to ensure only one bridges SCRs are triggered at one time. The RC snubber circuit is duplicated and connected in parallel with the second converters SCRs to protect them from the effects of dv/dt. Figure 7 shows the testing results of the design adaptation.

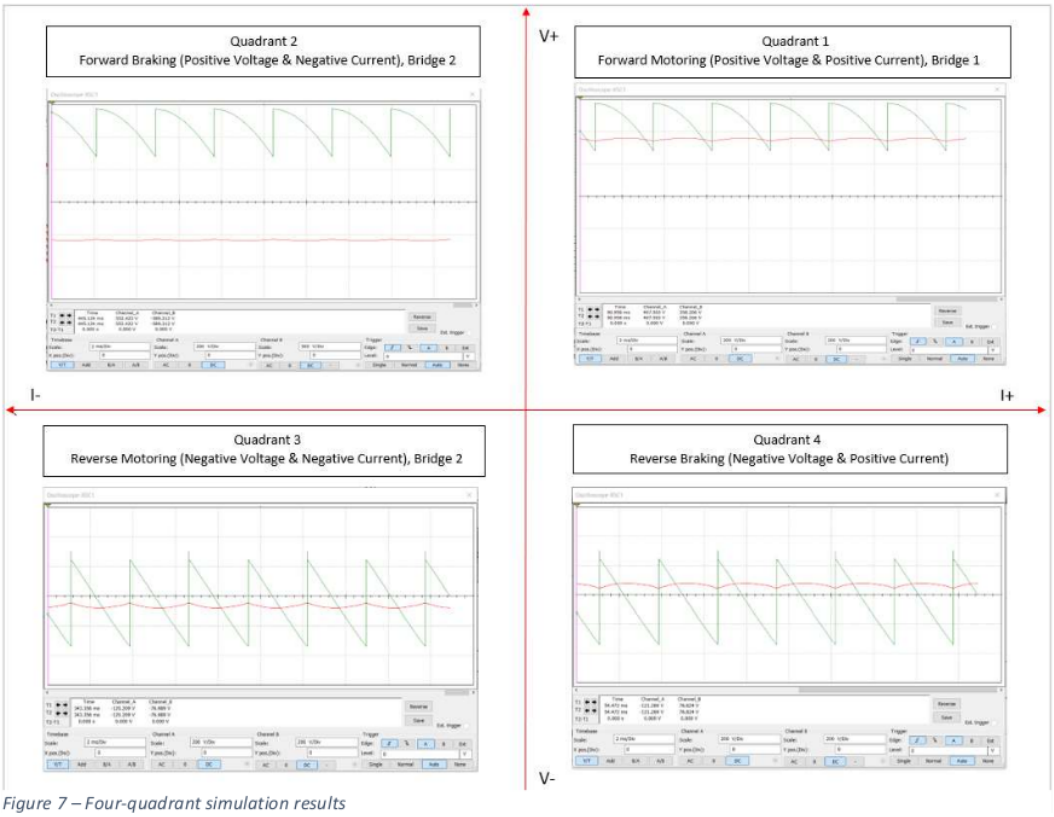


Figure 7 – Four-quadrant simulation results

Table 2 shows a comparison table of the results obtained from the test. The tests have proven successful with the correct waveforms being produced for each quadrant, agreeing with Krishnan's theory as seen in appendix 7.2.3 (Krishnan, 2001).

Four Quadrant Operation: Comparison between Theory and Simulation		
Quadrant	Expected Result	Simulation Result
I	Forward Motoring Positive Voltage & Positive Current	Forward Motoring Positive Voltage & Positive Current
II	Forward Generating Positive Voltage & Negative Current	Forward Generating Positive Voltage & Negative Current
III	Reverse Motoring Negative Voltage & Negative Current	Reverse Motoring Negative Voltage & Negative Current
IV	Reverse Generating Negative Voltage & Positive Current	Reverse Generating Negative Voltage & Positive Current

Table 2 - Four Quadrant Operation: Comparison between Theory and Simulation

.

3. Practical Investigations

3.1 Experimental Setup

The practical investigation is centred on an AC-DC motor system. The DC motor is controlled by a Siemens Three-Phase Sinamics DCM DC converter (6RA8013-6DV62-0AA0) for four-quadrant operation. The DC motor is mechanically connected to the AC motor by a belt and pulley, the AC motor is controlled by a Siemens S120 AC drive to act as a variable load for the DC motor. The experimental set-up consists of a Fail-Safe Siemens F Series S7-1511C PLC for controlling safety functions, communicating with the DCM and S120 for motor control through PROFINET, all user interface is possible via an HMI displaying all motor parameters.

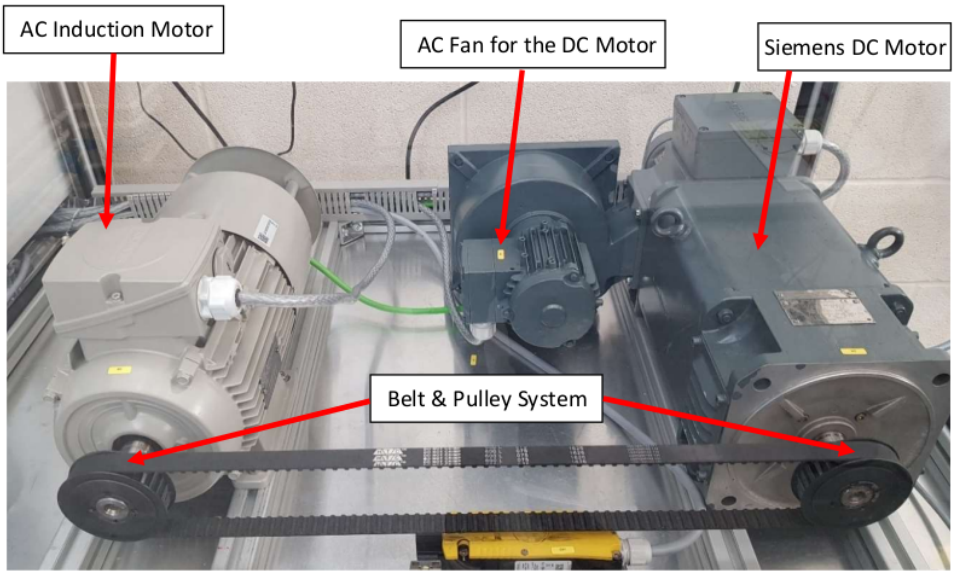


Figure 8 – Experimental set-up

A Picoscope is integrated to produce waveforms for Armature Voltage (V_a), Line Voltage (V_L), Armature Current (I) and Line Current (I_L), the Picoscope connections are seen in figure 34. A power analyser is used to obtain information on power usage in terms of True Power (kW), Reactive Power (kVAR) and Apparent Power (VA). The analyser also calculates the ratio between true power and total apparent power to determine the Power Factor (PF), the power analyser probes are connected to the DCM drives line conductors.

A detailed explanation of the control system and electrical schematics are seen in appendix 7.3.1, including explanations on the systems line filters, reactors, circuit protection and safety I/O, also displaying the test equipment connections.

3.2 Four Quadrant Operation

Figure 9 displays the HMI runtime graph of the DCMs four-quadrant operation, the blue trace represents speed whilst red represents torque. The relationship between these determines the quadrant of operation.

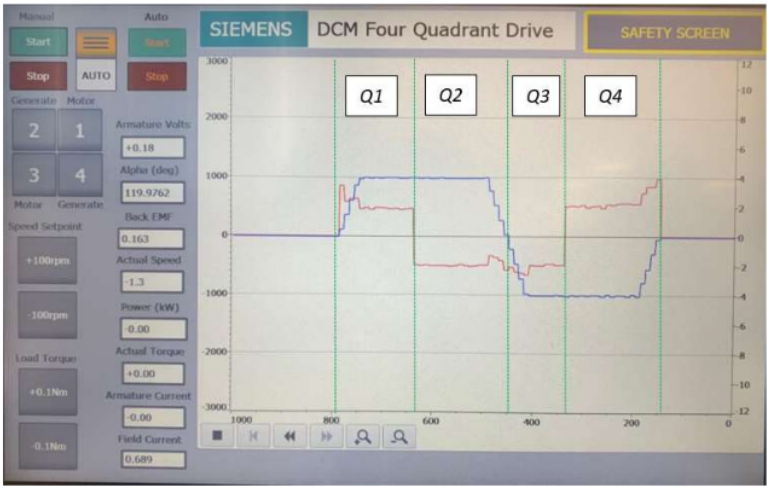


Figure 9 – HMI: Practical Four Quadrant Operation

Figure 10 displays the Picoscope graphs obtained simultaneously with the HMI graphs. The green trace represents line Voltage, brown represents line current, blue represents armature voltage and red represents armature current. Individual images of the Picoscope results are seen in appendix 7.3.2.

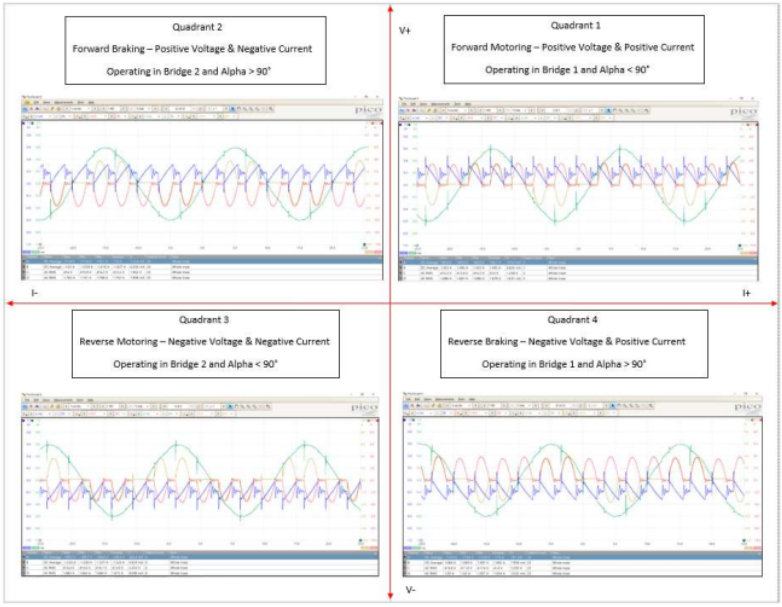


Figure 10 - Picoscope: Practical Four Quadrant Operation

Table 3 displays the expected result of the relationship between speed and torque compared to the HMI & Picoscope. Picoscope does not measure speed & torque, as it is an oscilloscope it measures voltage & current waveforms. Lander states that “speed of the motor is proportional to voltage; the current is proportional to torque” (1993). Table 3 proves Lander’s statement true, voltage and speed are always the same polarity, as are current and torque.

Four Quadrant Operation: Comparison between Theory and Practical			
Quadrant	Expected Result	HMI Result	Picoscope Result
I	Forward Motoring: Positive Speed & Positive Torque	Forward Motoring: Positive Speed & Positive Torque	Forward Motoring: Positive Voltage & Positive Current
II	Forward Generating: Positive Speed & Negative Torque	Forward Generating: Positive Speed & Negative Torque	Forward Generating: Positive Voltage & Negative Current
III	Reverse Motoring: Negative Speed & Negative Torque	Reverse Motoring: Negative Speed & Negative Torque	Reverse Motoring: Negative Voltage & Negative Current
IV	Reverse Generating: Negative Speed & Positive Torque	Reverse Generating: Negative Speed & Positive Torque	Reverse Generating: Negative Voltage & Positive Current

Table 3: Four Quadrant Operation: Comparison between Theory and Practical

Table 4 shows parameter values procured from the HMI during the 4 quadrant tests seen in appendix 7.3.2.

Four Quadrant Operation: Comparison of Motor Parameters in 4 Quadrants				
Parameters	Quadrant 1	Quadrant 2	Quadrant 3	Quadrant 4
Armature Voltage (Va)	184.63	173.26	-184.04	-172.97
Alpha (Degrees)	81.3648	116.2299	81.0571	115.3125
Back EMF (V)	180.013	179.12	-181.115	-179.231
Actual Speed (RPM)	997.9	998.5	-853.9	-1006.5
Power (kW)	0.28	-0.26	0.27	-0.28
Actual Torque (Nm)	1.96	-1.96	-1.95	2.09
Armature Current (Ia)	1.5	-1.5	-1.48	1.62
Field Current (If)	18.671	18.677	18.67	18.638

Table 4 - Four Quadrant Operation: Comparison of Motor Parameters in 4 Quadrants

Quadrant 1 shows both armature voltage and current are positive, delivering positive power. With positive current and a firing angle of 81.36° the DCM is operating in bridge 1. A back EMF smaller than the armature voltage along with positive speed and torque voltage indicates the motor is motoring forward.

Quadrant 2 indicates that the motor is forward braking. Armature voltage is positive; however, the back EMF is at a greater magnitude causing current to reverse polarity and flow back to the source, power and torque are also negative. A firing angle greater than 90° and negative current indicates it is operating in bridge 2. In

quadrant 2 the DC motor acts as a generator converting its kinetic energy produced whilst braking into electrical energy, this energy is returned to the source therefore the machine is regeneratively braking.

Quadrant 3 sees a negative armature voltage & current, producing positive power and operating in bridge 2. The firing angle is below 90˚, with a back EMF lower than the armature voltage and a negative torque this indicates the motor is motoring in reverse.

The transition from quadrant 3 to quadrant 4 sees the firing angle increase beyond 90˚, both current and torque are positive and the back EMF is greater than the armature voltage. The speed is negative, it is determined that the motor is regeneratively reverse braking. Quadrant 4 is often used as a method of quickly stopping the motion of a motor by reversing the armature terminals to induce a large back EMF to force the armature current to flow in the opposite direction, this method is known as “Plugging”.

It is concluded from the graphs and values obtained that current and torque are proportional, along with speed and voltage. It is determined that the DCMs bridge of operation is dependent on the current polarity, quadrants 1 and 4 operate in bridge 1 delivering positive current, whilst quadrants 2 & 3 operate in bridge 2 delivering negative current. Figures 39, 41, 43 and 45 in appendix 7.3.2 shows distortion on the line voltage, this is because the line voltage is momentarily short circuited each time the current commutates from one thyristor to another, this is expected as the supply impedance is never 0, most drives connected to secure supplies with circuit protection will not be affected by these spikes (Drury, 2013).

3.3 DC Motor Analysis – 3 different speed set-points

The DCM speed test is explained with screenshots in appendix 7.3.3. For this test the DC motors speed is variable and torque is constant. Table 5 displays values obtained from the HMI, Picoscope and Power Analyser during the test.

DCM Performance : 3 Speeds at a Constant Load Torque									
Motor Parameters	SP1 - 1001 RPM			SP2 - 1501 RPM			SP3 - 2000 RPM		
	HMI	Picoscope	P.A	HMI	Picoscope	P.A	HMI	Picoscope	P.A
Armature Voltage (Va)	185.95	184.5		273.13	274.4		362.26	363.4	
Firing Angle (α)	81.1285			71.1420			52.6410		
Back EMF (E)	178.754			270.961			361.522		
Speed (RPM)	1001.2			1501.0			2046.4		
Power (kW)	0.27		0.305	0.41		0.461	0.60		0.595
Actual Torque (Nm)	1.93			1.80			1.86		
Armature Current (Ia)	1.46	1.521		1.48	1.579		1.71	1.574	
Field Current (If)	18.683			18.677			18.693		
Power Factor (P.F)			0.256			0.491			0.501

Table 5 - DCM Performance : 3 Speeds at a Constant Load Torque

The values between the HMI and Picoscope for the three set-points are highly accurate with any errors being minor, these errors are likely due to the Picoscopes calibration or the DCMs scaling. The experiment proves the proportional relationship between armature voltage and speed, as the speed set-points are increased it clearly shows the armature voltage increases proving that the speed of a DC motor is dependent on its armature voltage. The inverse-relationship between firing angle and voltage is displayed, as the firing angle decreases from 81.12˚ the armature voltage greatly increases. The direct relationship between speed and back EMF is also seen, as they increase in-conjunction this is due to the rate of change of the induced electric field, as the speed increases so does the back EMF (Lalinsky, 2017).

As torque is the experiments constant, it does not change substantially. Armature current is not expected to change due to its proportional relationship with torque, however, set-point 3 shows an anomaly where the current increases by 200mA. As the current remains constant, the increase in speed increases the DC motors power consumption due to the voltage increase.

The power factor also increases as the speed increases, this is ultimately a consequence of speeds relationship with voltage (and voltages relationship with firing angle). An inversely-proportional relationship between power factor and firing angle is seen, as the speed increases so does the power factor. At a firing angle of 0˚, the silicon-controlled rectifiers power factor is close to unity, as the firing angle increases the rectifier becomes less and less linear, thus, increasing the lag between voltage and current and the currents harmonic content (Saracoglu, 2010).

Another method of calculating the armature voltage is through mathematical calculation, this is performed for set-point 1 as seen in appendix 7.3.3. This was calculated at 187.6V, an error of 1.65V to the HMI and 3.1V to the Picoscope, these errors are likely due to rounding and the calculation not accounting for any electrical losses.

3.3.1 Motor Constants

Using the cursor function on Picoscope seen in figure 11, the motor constants can be calculated.

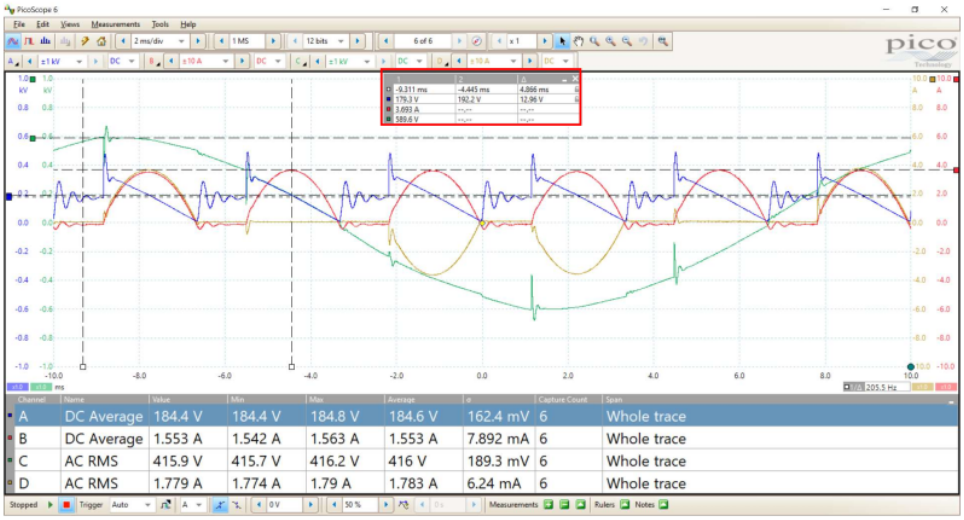


Figure 11 – Picoscope graph with cursors for motor constants

The dynamic resistance is calculated first:

$$Va = E + IaRa + L\frac{di}{dt}$$

$$At\ peak\ current, L\frac{di}{dt} = 0$$

Therefore, the equation is rearranged to find the armature resistance:

$$Ra = \frac{(Va - E)}{Ia} = \frac{12.96}{3.693} = 3.509342\Omega$$

This calculation is confirmed by substituting Ra in to the original equation, as it should total 192V:

$$Va = 179.3 + (3.693 \times 3.509342) = 192.26V$$

Using values obtained from the DCM displayed on the HMI seen in figure 12, further constants can be calculated:

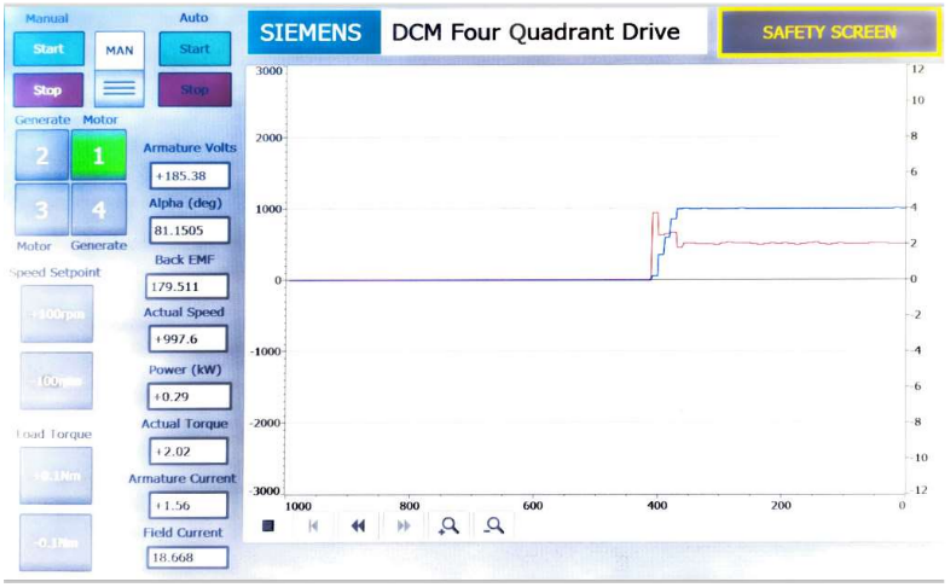


Figure 12 – Motor constants: HMI Values

The motor torque constant is calculated using the calculation below:

$$Kt = \frac{T}{Ia} = \frac{2.02}{1.56} = 1.295\text{Nm/A}$$

The motor back EMF constant is also calculated:

$$Ke = \frac{Ea}{\omega}$$

Where ω:

$$\omega = \frac{RPM}{2\pi} = \frac{997.6}{2\pi} = 158.77$$

Therefore Ke:

$$Ke = \frac{Ea}{\omega} = \frac{997.6}{158.77} = 6.283\text{V/Krpm}$$

3.4 DC Motor Analysis – 3 different torque set-points

The DC motor is analysed by varying the load torque to determine how its performance is affected under different load conditions within quadrant 1, a speed of 1900rpm is kept constant and current is continuous. Analysis is undertaken through Picoscope, a Power Analyser and DCM values displayed on the HMI as seen in appendix 7.3.4, table 6 displays the results obtained from the tests.

DCM Performance: 3 Torque values at a constant speed									
Motor Parameters	Set-point 1 – 6.12Nm			Set-point 2 – 4.70Nm			Set-point 3 – 3.60Nm		
	HMI	Picoscope	P.A	HMI	Picoscope	P.A	HMI	Picoscope	P.A
Armature Voltage (Va)	355.8	355.2		353.17	354.1		352.80	352.2	
Firing Angle (α)	48.21			49.5483			52.8278		
Back EMF (E)	336.322			344.004			339.384		
Speed (RPM)	1900.2			1904			1904.3		
Power (kW)	1.69		1.676	1.33		1.336	1.01		1.027
Actual Torque (Nm)	6.12			4.70			3.6		
Armature Current (Ia)	1.69	4.671		3.65	4.192		2.78	3.829	
Field Current (If)	18.633			18.700			18.670		
Power Factor (P.F)			0.581			0.559			0.533

Table 6 - DCM Performance: 3 Torque values at a constant speed

The proportional relationship between armature current and torque is displayed, as the torque is increased the current drawn also increases, the current increase is required to produce the extra torque needed to maintain the speed set-point at the increased load (Collins, 2016). As the speed set-point remains constant, when the load torque increases the motor requires greater power as seen above as confirmed by the power analyser and HMI.

Most motor characteristics remain unchanged throughout the tests, with miniscule changes at most. This proves that current does not have as great of an effect on the motor characteristics as voltage does, as current is only affecting torque and power as seen in table 6.

The theory that power is a product of rotational speed and torque is confirmed in table 6. As the torque increases and the speed is kept constant the Power increases, as the load torque is increased the DCM is supplying a greater power rating due to the increase in torque.

The values obtained from the power analyser are highly accurate compared to the HMI value, as is the Picoscope voltage compared to the HMI. However, the current value obtained by the Picoscope displays anomaly's which are unaccounted for.

3.5 Analysis of the DCMs Performance

The DCM performed proficiently throughout the tests. All values obtained throughout the experiments were confirmed by theory or simulation, in turn proving the legitimacy of the experiment. The data function was exceptional in writing data to the PLC, allowing for values to be compared to theory adding further evidence throughout the tests. The efficiency of the DCM was demonstrated when cycling through the quadrants, it operated in all four quadrants seamlessly.

It was found throughout the test that the DCM has a negative impact on the supplies power factor when operating a low speed. This is a drawback of using converter-fed DC drives at low speed as it causes the supply current to lag the supply voltage, in turn lowering the power factor.

For the performance of the DC motor throughout the practical tests, it was found that the field current is constantly around 18A. This is due to the separately-excited DC motor having a regulated field voltage, therefore the current is fixed (Linquip, 2021)

4. Overall Conclusions and Recommendations

From an overall point of view in terms of the calculations, results and observations undertaken, this report has proven successful.

Comprehensive research was undertaken based around the Siemens DCM DC converter, specifically the control techniques and design features where it is found that the DCM (6RA8013-6DV62-0AA0) controls the field and armature of variable speed DC motors up to 30MW, the power circuit consists of two thyristor bridges connected in anti-parallel across the DC motor allowing for four-quadrant control. The DCM was found to be a '*circulating-current free'* converter which removes the need for circulating-current reactors between the load and rectifiers, enabled by control functions to only enable one bridge to conduct at a time, creating a torque-free dead time of 10ms before enabling the other bridge sensed by the drives control elements. Siemens have developed the control unit to allow for ease of commissioning, also implementing various I/O and communications functionalities such as PROFINET and PROFIdrive for seamless connection between PLCs. Research into the control techniques employed in the drive found that the DCM employs closed-loop control for current and speed feedback allowing for accurate control through PI controllers. For four-quadrant operation it is found that auto-reversal control is implemented to ensure the reversal of torque is safe to allow for gate firing. Further research into applications of DC converters found that Siemens DCM drives are commonly used in retrofitting applications such as Ward-Leonard systems and traction applications. However, AC drives now offer the same control as DC motors with reduced maintenance requirements and DC choppers also offer better performance in applications such as mass rapid transit systems. The selection of drives was explored, it was found that there are many requirements when choosing a drive, including customer needs, infrastructure and performance level.

The simulation was found to be an accurate method of modelling a separately-excited DC motor, the fully-controlled three-phase rectifier model is modelled to a physical drive, including the phase-angle controller for gate control and RC snubbers to protect the drive from effects of transients. The simulation allowed for accurate testing of the DC motors armature voltage at three different firing angles. It was concluded that as the firing angle increases the armature decreases, this is due to greater sections of the input waveform are 'chopped' when the firing angle increases. Mathematical equations were undertaken to prove the validity of Multisim, it was found that Multisim is highly accurate as miniscule errors were found between simulation and calculation, it was deduced that these errors are likely due to rounding and Multisims inclusion of voltage-drop across the SCRs.

A design adaptation based on Krishnan & Ramaswami's paper was implemented on the simulation, by adding an extra bridge of SCRs in anti-parallel with the load enabled control in four-quadrants, the addition of switching elements allowed the simulation to be based on a circulating-current free drive such as the Siemens DCM, allowing for load and EMF for different quadrant control. Thorough testing was undertaken, using Krishnans theory of operation as a comparison, it was found that all four-quadrants produced the correct waveform responses, proving the accuracy of the adaptation.

The practical experiment undertaken based on the AC-DC motor system, specifically focused on the Sinamics DCM were successful. Various test equipment was used to obtain readings for the systems characteristics, a Picoscope is used to measure armature current, armature voltage, line current and line voltage, a power analyser was also used to obtain information on the systems power ratings, specifically power consumption and power factor, the HMI displayed all of the relevant information of the drive's parameters. The first practical saw the DCM operated in all four quadrants as the AC drive is run as a variable load coupled to the DCM, comparisons undertaken between Lander's theory. The HMI result and Picoscope result displayed the continuities between them, also proving the proportional relationships between current & torque and voltage & speed proving the relevant links between theory and practical. The values from the HMI during testing were tabulated and compared, showing that DC motors characteristic operate in a set manner for each quadrant.

Further experiments undertaken to analyse the DCMs performance also proved relevant to theory, 3 speed set-points were applied to the DCM to determine how it operated under 3 speeds at a constant load torque. This experiment proved the relationship between speed and armature voltage, as the speed set-point was increased so did the armature voltage. The inverse relationship between firing angle and voltage was also proven, correlating with the simulated results that as the firing angle increases the armature voltage falls. It was also displayed that as the DC motors speed increases the power factor increases closer to unity, this is due to the SCRs linearity which is directly affected by the SCRs firing angle, therefore it is deduced that the greater the speed of the DC motor, the greater the power factor, proving that it is inefficient to control motors at low speeds by dc converters.

The final experiment was focused on the DCMs response to three different torque values, this proved torques proportional relationship with armature current, correlating with both theory and simulations, proving the reliability of the three methods. Further theories were confirmed, such as the theory that power is a product of torque and rotational speed.

In conclusion, the research, simulation and experiments were all highly successful. All theories produced were proven by the simulation and experiments with substantiating evidence. The theories of various engineers were tested, with theories of over 30 years old being confirmed by new equipment demonstrating the relevance of their theories.

As a recommendation, further practical experiments could be conducted by controlling an AC induction motor and a DC stepper motor within the four quadrants, this would allow for comparison of performance to be made between the DCM and other machines. This would enable further examination into the performance of each method, and how they compare. A further recommendation would be to re-perform the torque set-point tests to obtain more accurate current values on the Picoscope enabling true analysis to be undertaken.

5. Team Working and Health & Safety Precautions

Due to the global pandemic, team working was limited. All HSE guidelines were followed and a safe working environment was provided by the lecturer when performing experimental activities. Team working was only required for the practical task, all other sections were individual tasks, in turn minimising the contact between students limiting the potential spread of coronavirus.

For the practical experiment, the author was in a group of three. Their task was to run the machine, obtain screenshots of the HMI, Picoscope and Power Analyser. The author also used the Picoscope cursors to find out information required for analysis and calculations. By having one person operating the machine this eliminated the potential of multiple people touching the pushbuttons and HMI.

All workstations were sanitised before and after use and all relevant PPE including face masks were worn during the practical experiment where there is close contact.

.

6. Works Cited

ABB, 2020. *How drives can unlock hidden value in your operations.* [Online]
Available at: https://new.abb.com/drives/drive-selection
[Accessed 05 01 2022].

Collins, D., 2015. *FAQ: What are DC shunt motors and where are they used?.* [Online]
Available at: 2021
[Accessed 01 05 2021].

Collins, D., 2016. *Lenz's Law and Back EMF.* [Online]
Available at: https://www.motioncontroltips.com/lenzs-law/
[Accessed 22 12 2021].

Drury, A. H. a. B., 2013. Electric Motors and Drives. In: *Fundamentals, Types, and Applications.* Oxford: Elsevier, p. 125.

Drury, A. H. a. B., 2013. Electric Motors and Drives Fourth Edition. In: Newnes, ed. *Fundamentals, Types, and Applications.* Oxford: Elsevier, p. 124.

eeeguide, 2016. *https://www.eeeguide.com/four-quadrant-operation-of-motor-drive/.* [Online]
Available at: https://www.eeeguide.com/four-quadrant-operation-of-motor-drive/
[Accessed 05 01 2022].

ElectronicsTutorials, 2019. *Thyristor Tutorial.* [Online]
Available at: https://www.electronics-tutorials.ws/power/thyristor.html
[Accessed 02 05 2021].

Hughes, A., 2013. Conventional DC Motors. In: *Electric motors and drives: Fundamentals, Types, and Applications..* s.l.:Newnes, p. 437.

Kharagpur, 2015. *Module 2: AC to DC Converters,* s.l.: EE ITT.

Krishnan, R., 2001. Electric Motor Drives. In: M. J. Horton, ed. *Modelling, Analysis and Control.* New Jersey: Prentice Hall, p. 46.

Lalinsky, J., 2017. *Why does more rapidly changing magnetic field induce greater EMF?.* [Online]
Available at: https://physics.stackexchange.com/questions/326962/why-does-more-rapidly-changing-magnetic-field-induce-greater-emf
[Accessed 22 12 2021].

Lander, C. W., 1993. Power Electronics. In: McGraw-Hill, ed. *Power Electronics.* Leicester: McGraw-Hill, p. 360.

Lander, C. W., 1993. Power Electronics. In: C. W. Lander, ed. *Inverter.* Leicester: McGraw-Hill, p. 418.

Lander, C. W., 1993. Power Electronics and Drives. In: McGraw-Hill, ed. *Rectifying Circuits .* Berksire : McGraw-Hill, p. 15.

Lawson, J., 2019. *Top 5 factors to consider when selecting a drive controller.* [Online]
Available at: https://www.engineerlive.com/content/top-5-factors-consider-when-selecting-drive-controller
[Accessed 05 01 2022].

Linquip, 2021. *Separately Excited DC Motor.* [Online]
Available at: https://www.linquip.com/blog/separately-excited-dc-motor/
[Accessed 13 01 2022].

Omron, 2013. *MX2 Born to drive machines,* Tokyo: Omron.

PROFIBUS, 2019. *PROFIdrive & Encoder.* [Online]
Available at: https://www.profibus.com/technology/profidrive
[Accessed 03 01 2022].

profibus, 2020. *Interoperable, Standardized and Manufacturer-Independent Interface.* [Online]
Available at: https://www.profibus.com/technology/profidrive/overview
[Accessed 05 01 2022].

Ramaswami, T. K. &. B., 1976. *Speed control of d.c motor using thyristor dual converter,* s.l.: IEEE.

Rashid, M., 2018. Power Electronics Handbook. In: A. Valutkevich, ed. *9.2.12 Dual Converters.* Oxford: Elsevier, p. 250.

Rashid, M. H., 2013. Power electronics: devices, circuits and applications.. In: s.l.:Pearson Education, p. 1014.

Rashid, M. H., 2014. Power Electronics. In: *Devices, Circuits and Applications.* Essex: Pearson, p. 722.

Rashid, M. H., 2014. *Power Electronics - Devices, Circuits and Applications.* Fourth Edition ed. Essex: Pearson.

Rashid, M. H., 2018. Power Electronics Handbook. In: *Dual Converters.* Oxford: Elsevier, p. 250.

S., N., 2014. *Single phase half controlled bridge converter,* s.l.: iitb.

Saracoglu, B., 2010. Supply power factor and load current harmonic performance improvement of three phase AC voltage controller. *Power factor relationships in conventional scheme,* 1(1), p. 7.

Schneider, 2018. *To what standards do the A class and B class filters correspond in the variable speed drives?.* [Online]
Available at: https://www.se.com/uk/en/faqs/FA28058/
[Accessed 05 01 2022].

Semiconductors, N., 2012. *BTW42-600R.* [Online]
Available at: https://www.arrow.com/en/products/btw42-600r/nxp-semiconductors
[Accessed 06 01 2022].

Shidling, C., 2020. *What is Quadrant Diagram, Explain The Quadrant Diagram For Hoist Drive System.* [Online]
Available at: https://www.cselectricalandelectronics.com/what-is-quadrant-diagram-explain-the-quadrant-diagram-for-hoist-drive-system/
[Accessed 05 01 2022].

Siemens, 2012. *Sinamics DCM DC Converter.* [Online]
Available at: https://snumam.com.br/template/pw-pdf/56-dcm-converter-0212-en.pdf
[Accessed 05 01 2022].

Siemens, 2013. *Closed-loop control application for a Ward-Leonard block.* [Online]
Available at: https://cache.industry.siemens.com/dl/files/187/54140187/att_66606/v1/Application_Ward-Leonard-Block.pdf
[Accessed 04 01 2022].

Siemens, 2013. *DRIVE-CLiQ interface.* [Online]
Available at: https://assets.new.siemens.com/siemens/assets/api/uuid:d52d5d92-5c83-4b6f-85b5-7d0fd3541fa9/drive-cliq-interface-flyer.pdf
[Accessed 05 01 2022].

Siemens, 2014. *Sinamics Drives Catalog D 23.1,* s.l.: Siemens.

Siemens, 2015. *SINAMICS drives.* [Online]
Available at: https://cache.industry.siemens.com/dl/files/240/109478240/att_851818/v1/manual-DC-Converter_en.pdf
[Accessed 05 01 2022].

Siemens, 2018. *Sinamics DCM Control Module,* s.l.: Siemens.

Siemens, 2021. *Technical Support.* [Online]
Available at: https://new.siemens.com/global/en/company/sustainability/education/sce/technical-support.html
[Accessed 05 01 2022].

TeX, 2018. *SCR (aka thyristor) symbol in TikZ circuit.* [Online]
Available at: https://tex.stackexchange.com/questions/430193/scr-aka-thyristor-symbol-in-tikz-circuit
[Accessed 02 05 2021].

Wildi, T., 2014. Electrical Machines, Drives and Power Systems. In: Essex: Pearson, p. 584.

7. Appendix

7.1 Appendix for Section 1

7.1.1 Sinamics Application Class

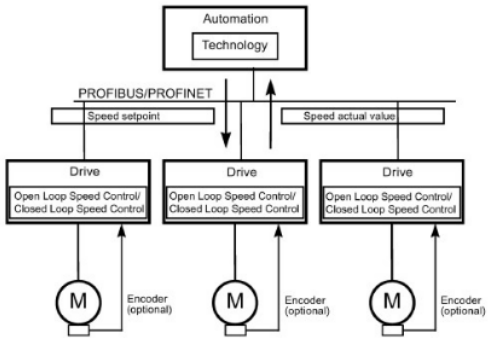


Figure 13 – Sinamics DCM Application Class 1 (Siemens, 2015)

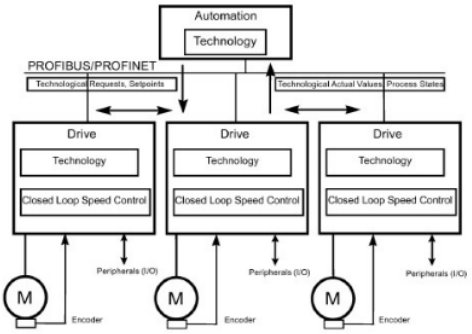


Figure 14 – Sinamics DCM Application Class 2 (Siemens, 2015)

7.1.2 Siemens Sinamics DCM control circuit

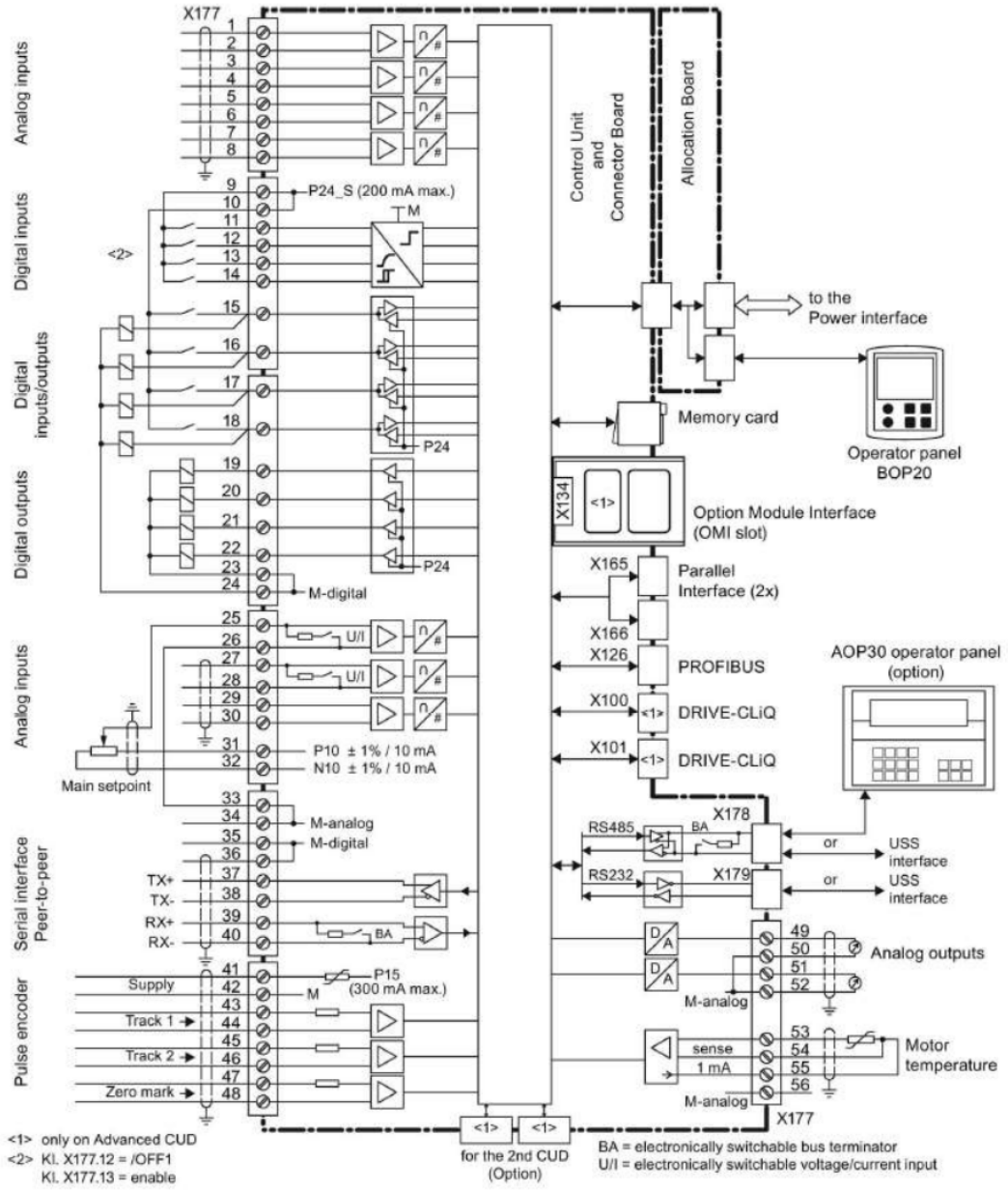


Figure 15 – Sinamics DCM Control Circuit (Siemens, 2012)

7.1.3 – Industrial hoist system explanation

In industrial hoist systems, a four-quadrant drive is required for 4 different scenarios. In quadrant 1, the loaded cage weighs greater than the counterweight. The upward motion of the motor means that the motors direction is anti-clockwise with the load torque operating in the opposed direction of motor motion, therefore to pick up the cage up speed and torque must be positive by forward motoring. The load is removed and the hoist is moved back up, as the counterweight is heavier than the cage it can move at an excessive speed, this is prevented by producing a negative torque to oppose the positive speed known as forward braking in quadrant 2. To hoist an empty cage downwards the load torque of the counterweight outweighs the cage, therefore the motor torque must match the motor rotation both being negative causing the motor to operate in reverse motoring in quadrant 3. Quadrant 4 sees the loaded cage being pulled down; therefore, speed needs to be limited due to the load weight, here speed is negative, therefore a positive torque is produced to decrease the motor speed. By using a four-quadrant DC drive it removes the need for mechanical brakes during operation allowing for reduced system complexity (Shidling, 2020).

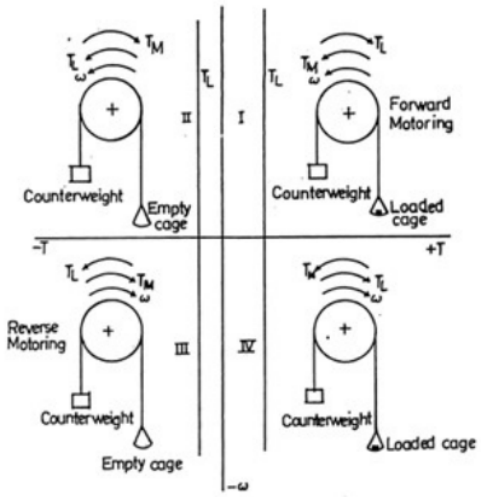


Figure 16 – Four quadrant operation for hoisting (eeeguide, 2016)

7.2 Appendix for Section 2

7.2.1 Simulation Thyristor Data Sheet

이 그림이 존재하지 않음

NXP Semiconductors

BTW42-600R

Silicon Controlled Rectifiers - SCRs

SCR 600V 16A(RMS) 150A 3-Pin TO-64

See all *Silicon Controlled Rectifiers - SCRs by NXP Semiconductors*

Share

Download Pricing

Product Technical Specifications

EU RoHS	**Supplier Unconfirmed**
ECCN (US)	**EAR99**
Part Status	**Unconfirmed**
Automotive	**No**
PPAP	**No**
Maximum Rate of Rise of Off-State Voltage (V/us)	**500**
Maximum Rate of Rise of On-State Current (A/us)	**50**
Maximum Gate Trigger Voltage (V)	**1.5**
Maximum Gate Trigger Current (mA)	**50**
Surge Current Rating (A)	**150**
Maximum Holding Current (mA)	**75**
Repetitive Peak Reverse Voltage (V)	**600**

Figure 17 – Datasheet for BTW42-600R SCR ((Semiconductors, 2012)

7.2.2 – Simulation Calculations and Waveforms

Figure 18 shows the phase-angle controllers firing angle set to 0˚. At this firing angle V_{MAX} is found on the waveforms found on the Multisim oscilloscope connected across the output of the load. At 0˚ V_{MAX} is found to be 575.466.

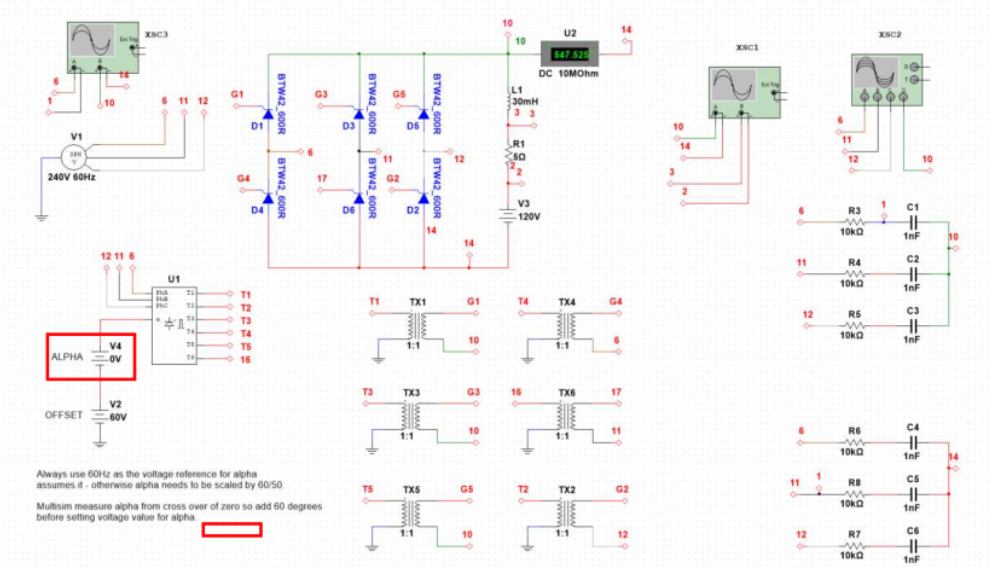


Figure 18 – Simulation Testing: Firing Angle set to 0˚

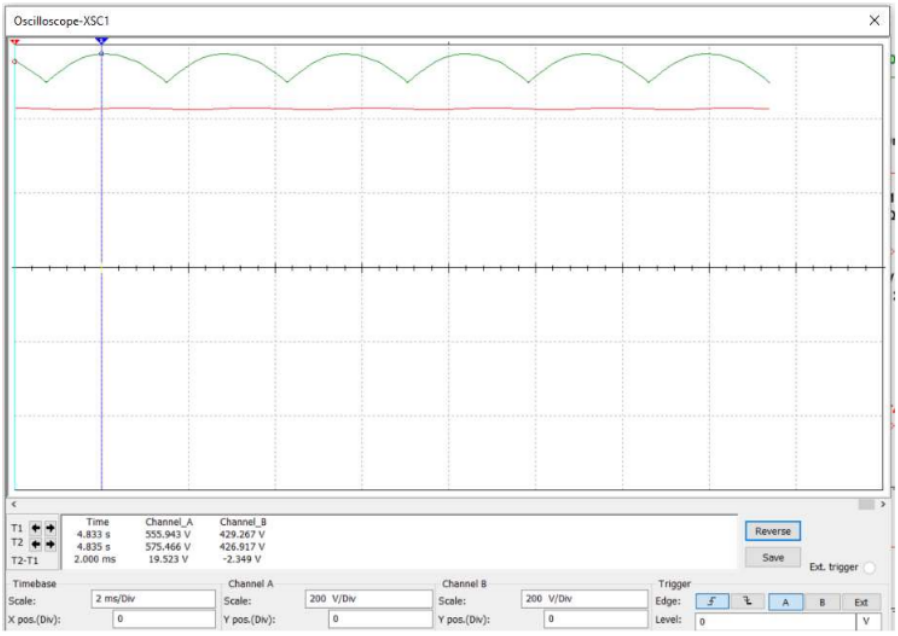


Figure 19 - Simulation Testing: Vmax found at 575.466V

Test 1 - 10˚ Firing Angle

Figure 20 shows that for the first test the firing angle is set at 10˚. At this firing angle the armature voltage is read by the voltmeter at 540.478. Figure 21 shows that current is continuous at a 10˚ firing angle.

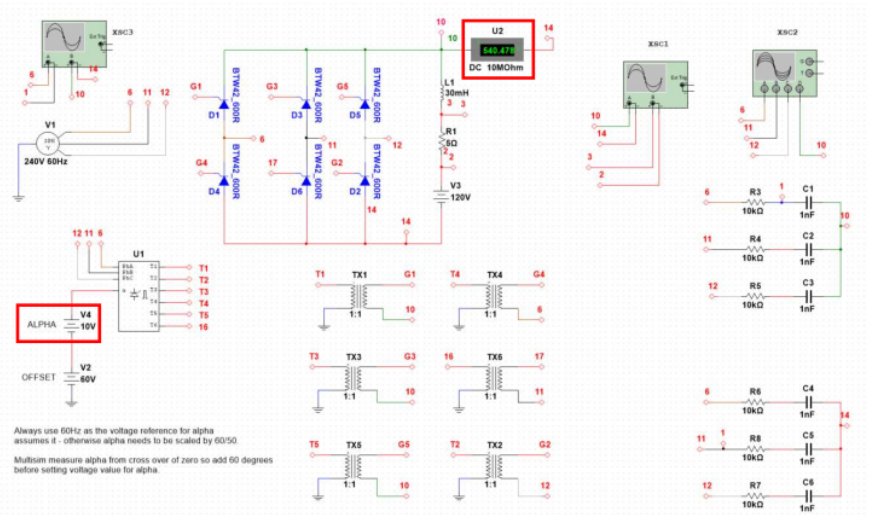


Figure 20 - Simulation Test 1: 10˚ Degree Firing Angle

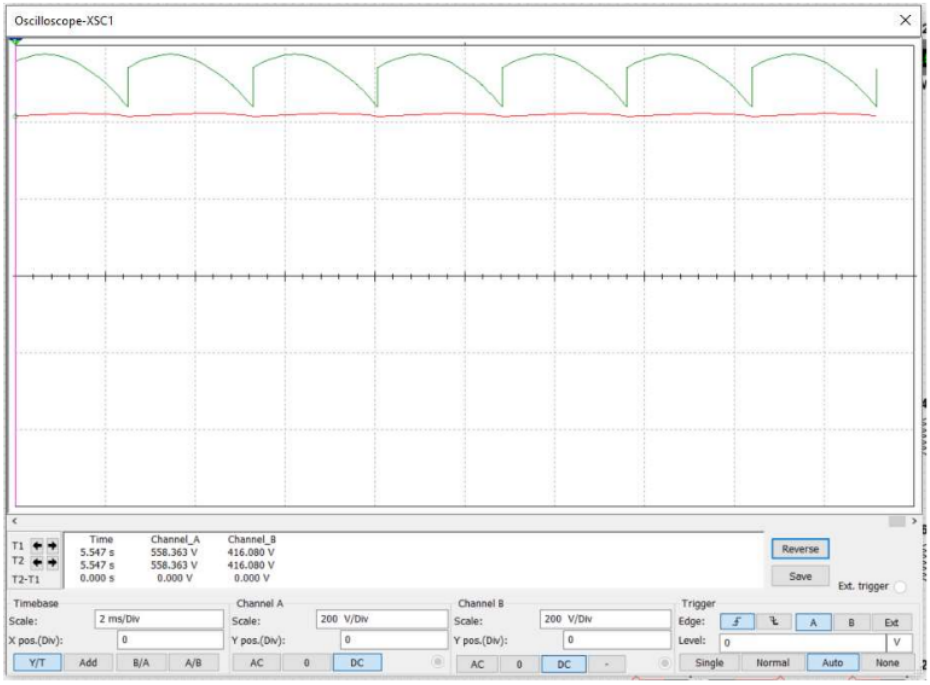


Figure 21 - Simulation Test 1: Armature Voltage & Current at 10˚

The accuracy of Multisim is confirmed using the equation below:

$$V_{mean} = \frac{3 \times V_{max}}{\pi} \times Cos(\propto)$$

Where Vmax = 575.466V and $\propto$ = 10˚:

$$V_{mean} = \frac{3 \times 575.466}{\pi} \times Cos(10) = 541.180$$

Test 2 - 20˚ Firing Angle

The second test was set at a firing angle of 20˚. Figure 22 shows the armature voltage at this angle determined by the voltmeter, it is seen that the average armature voltage is 516.129V. At this firing angle the current is still continuous as seen in figure 23.

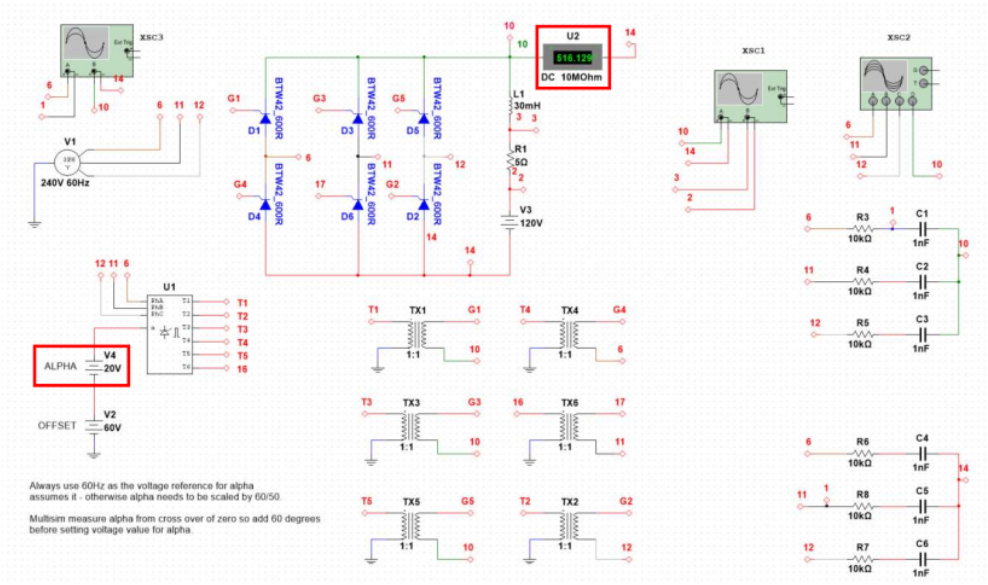


Figure 22 - Simulation Test 2: 20˚ Degree Firing Angle

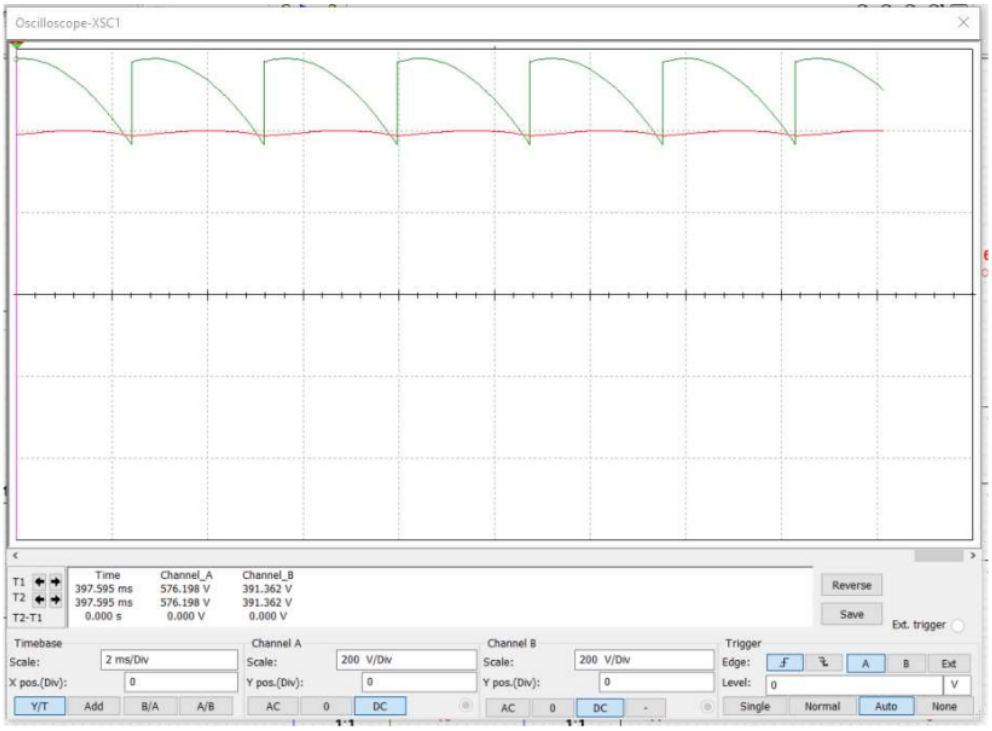


Figure 23 - Simulation Test 2: Armature Voltage & Current at 20˚

The accuracy of Multisim is determined by the same equation used in the 10˚ calculation:

$$V_{mean} = \frac{3 \times V_{max}}{\pi} \times Cos(\propto)$$

Where Vmax = 575.466V and ∝ = 20˚:

$$V_{mean} = \frac{3 \times 575.466}{\pi} \times Cos(20) = 516.388V$$

Test 3 - 30˚ Firing Angle

The final firing angle test is seen in figure 24, this test is set at 30˚. This figure shows that the average armature voltage is 475.598V. The armature voltage and current waveforms are seen in figure 25, again it is seen that current is continuous at this firing angle.

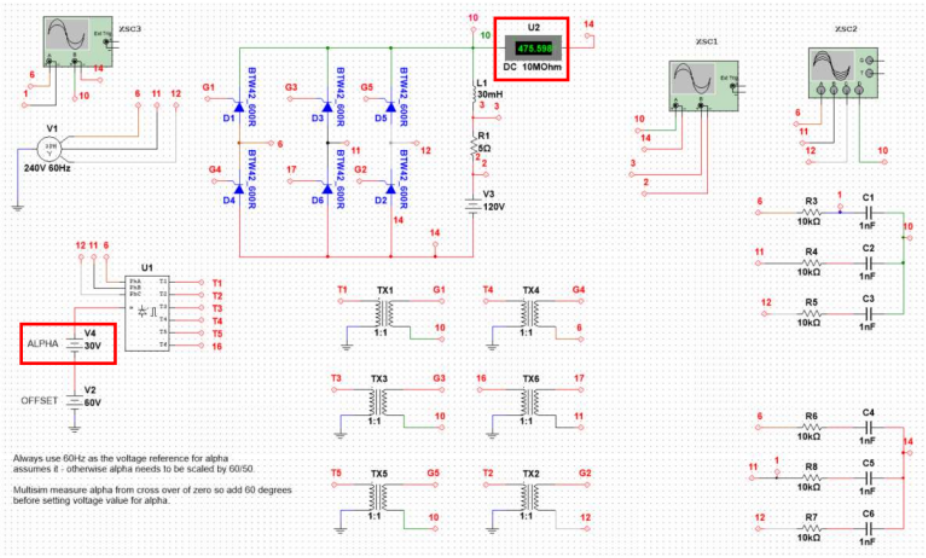


Figure 24 - Simulation Test 3: 30˚Degree Firing Angle

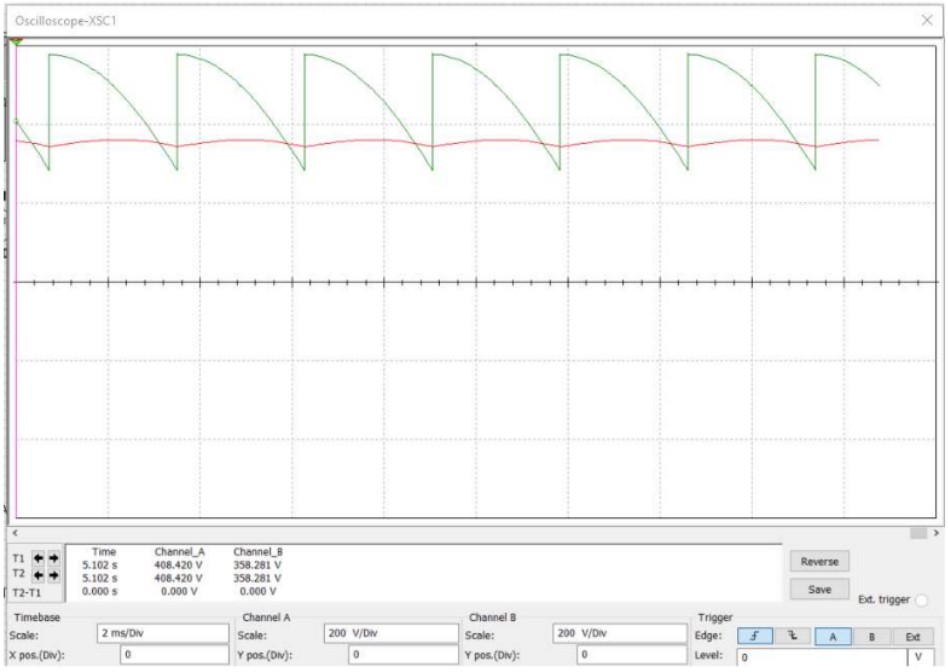


Figure 25 - Simulation Test 3: Armature Voltage & Current at 30˚

The accuracy of Multisim is confirmed using the equation below:

$$V_{mean} = \frac{3 \times V_{max}}{\pi} \times Cos(\propto)$$

Where Vmax = 575.466V and $\propto = 30^{\circ}$:

$$V_{mean} = \frac{3 \times 575.466}{\pi} \times Cos(30) = 475.907V$$

7.2.3 – Design and Adaptation for Three-phase fully-controlled dual bridge converter

Figure 26 shows the main control circuit of the design adaptation, a second bridge is connected in anti-parallel with the load, enabling operations in bridge 2 and 3. Switches have been added between bridges, reducing the potential of circulating currents between bridges. Switches have also been added to allow for the back EMFs polarity to be reversed.

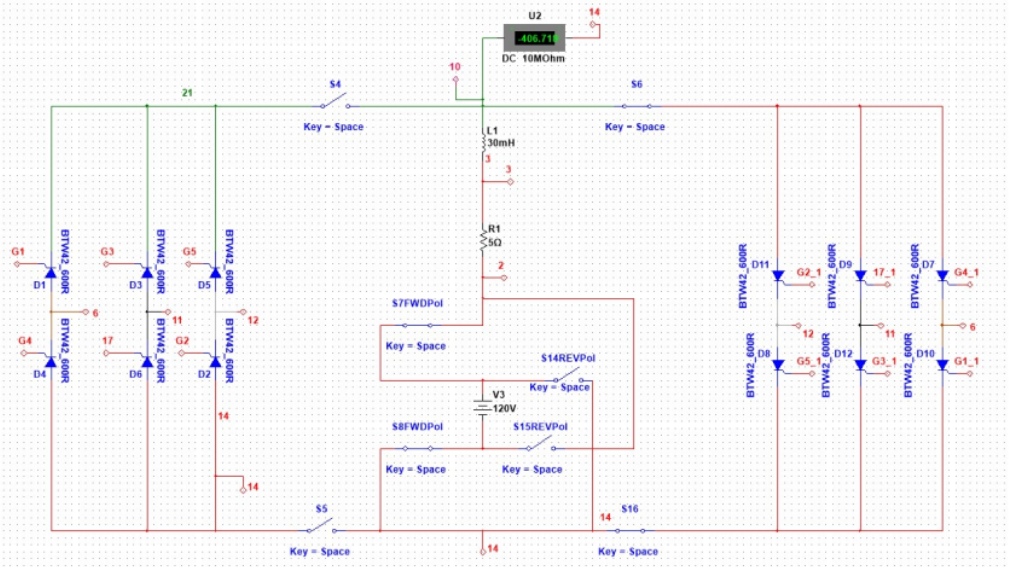


Figure 26 – Main Circuit: Three-phase fully-controlled dual bridge converter adaptation

Figure 27 shows the auxiliary circuit of the adapted circuit, a switch has been added on the transformers secondary to have control over which bridge is triggered, this is essentially working as a master controller. The RC snubber circuit has been duplicated and connected in parallel with the thyristors of the second bridge.

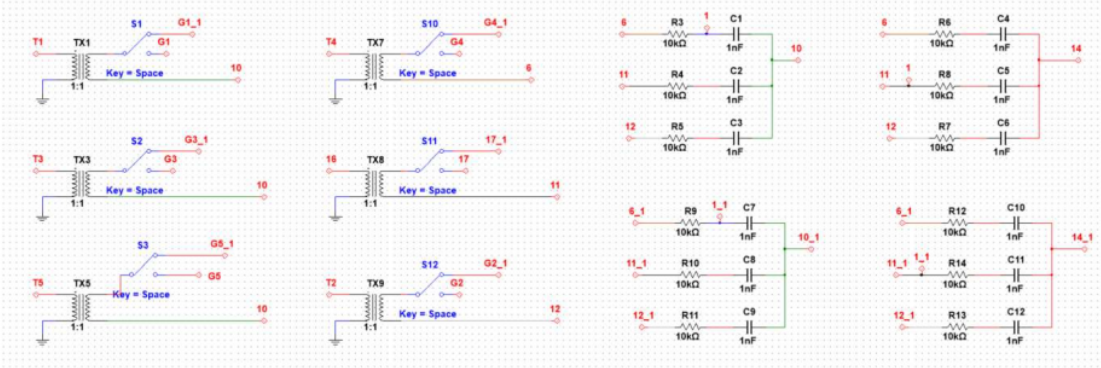


Figure 27 - Auxiliary Circuit: Three-phase fully-controlled dual bridge converter adaptation

7.2.4 Krishnans Theory of Four quadrant operation

Figure 28 displays Krishnans theory of the relationships between Speed, Torque and Power in each quadrant. Krishan relates '*Forward Regeneration*' to quadrant 4 and '*Reverse Regeneration*' to quadrant 2. However, for this paper these are swapped with quadrant 2 relating to '*Forward Regeneration*' and quadrant 4 to '*Reverse Regeneration*'.

Function	Quadrant	Speed	Torque	Power Output
Forward Motoring (FM)	I	+	+	+
Forward Regeneration (FR)	IV	+	−	−
Reverse Motoring (RM)	III	−	−	+
Reverse Regeneration (RR)	II	−	+	−

Figure 28 – Krishnans theory of four quadrant operation (Krishnan, 2001)

7.2.5 – Testing for Three-phase fully-controlled dual bridge converter

In quadrant 1 both armature voltage & armature current are positive, the firing angle is below 90˚ and the converter is operating in bridge 1. It is determined that the DC motor is operating in forward motoring mode (Figure 29).

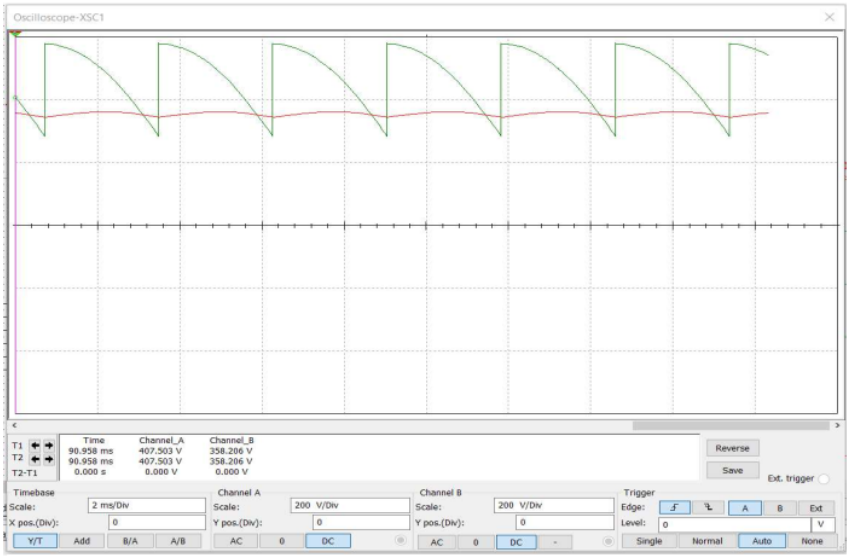


Figure 29 - Simulation Adaptation: Quadrant 1

In quadrant 2 armature voltage is positive & armature current is negative, the firing angle is beyond 90˚ and the converter is operating in bridge 2. It is determined that the DC motor is operating in forward braking mode (Figure 30).

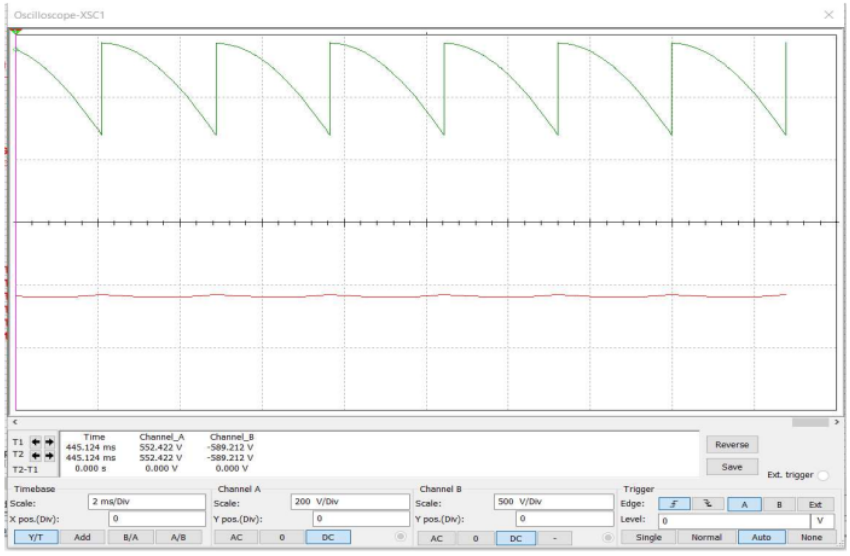


Figure 30 - Simulation Adaptation: Quadrant 2

In quadrant 3 both armature voltage & armature current are negative, the firing angle is below 90° and the converter is operating in bridge 2. It is determined that the DC motor is operating in reverse motoring mode (Figure 31).

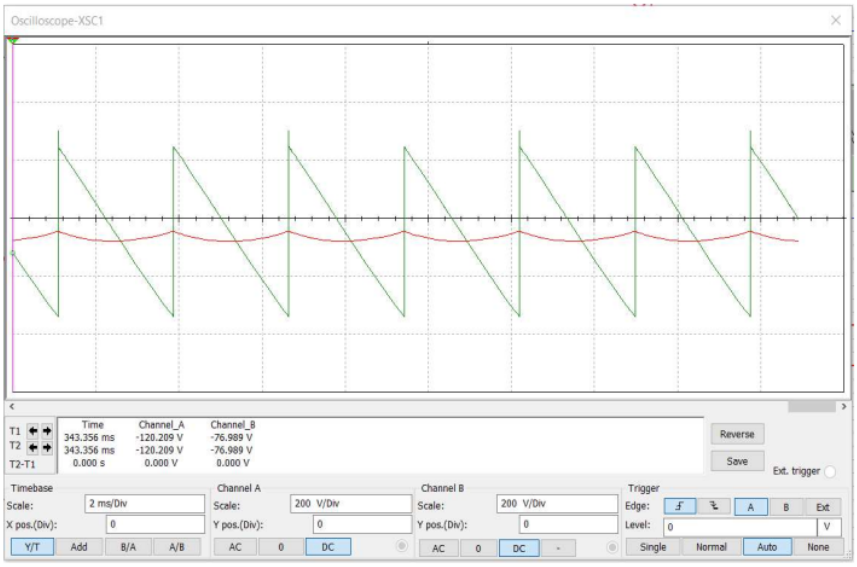


Figure 31 - Simulation Adaptation: Quadrant 3

In quadrant 4 armature voltage is negative & armature current is positive, the firing angle is beyond 90° and the converter is operating in bridge 1. It is determined that the DC motor is operating in reverse braking mode (Figure 32).

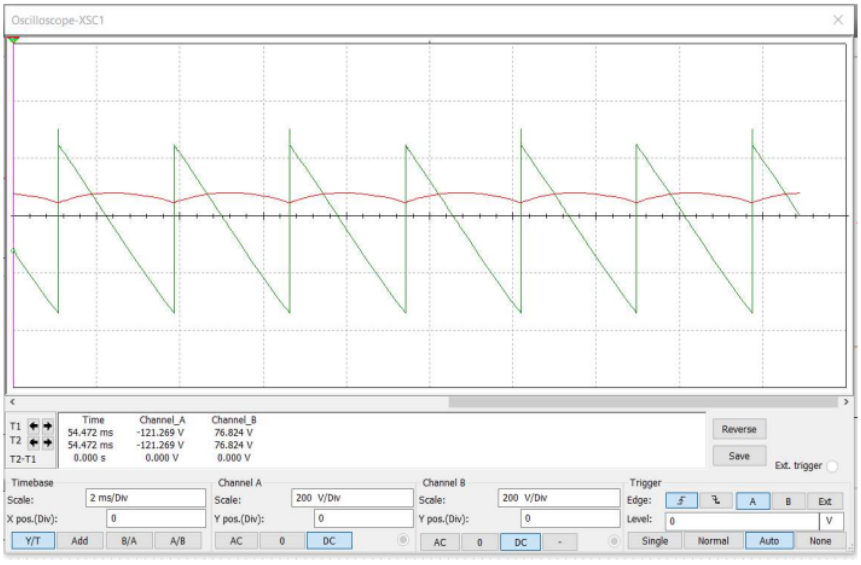


Figure 32 - Simulation Adaptation: Quadrant 4

7.3 Appendix for Section 3

7.3.1 Explanation of experimental set-up, drive connections and measuring equipment

The experiment is based upon the Siemens Three-Phase Sinamics DCM DC converter for four-quadrant drives (6RA8013-6DV62-0AA0), showing its ability to perform within the four motor quadrants. The DC motor is mechanically connected to the DC motor via a belt and pulleys acting as its variable load. The experimental set-up consists of a Siemens F Series S7-1511C PLC which communicates with the DCM Drive which controls the DC motor, a Sinamics S120 AC Drive for the AC motor and a TP1200 Comfort Panel HMI through PROFINET industrial fieldbus. An important function carried out by PROFINET within this system is communicating between the drives and the PLC through an acyclic routine whereby parameters are read by the PLC from the drives and written to the drives by the PLC, allowing for key system information such as armature voltage, current, speed, torque and firing angles to be displayed. PROFINET is also used to send the torque set-point to the AC Drive and Speed set-point to the DC drive.

The DCM DC Converter operates as a single unit, it is powered by a 415VAC Three-Phase supply which feeds a commutating reactor which is essentially connected in series with the drive's commutation capacitor, forming an efficient resonant circuit, producing a current oscillation which commutates the conducting SCR. The DC motor is output circuit of the DCM. The DC Drive is coupled with an AC Motor Fan for cooling purposes.

However, the S120 requires additional units. The Sinamics S120 control unit (6SL3040-1MA01-0AA0) provides the control section for the AC motor, communicating with the PLC via PROFINET. The control unit is coupled with a S120 Smart Line Module (6SL3130-6AE15-0AB1), this is a regenerative unit allowing for stable line-commutated regenerative feedback through IGBTs providing for minimal switching losses allowing for a high percentage of the power unit current to be utilised. The Smart Line module is supplied with 415VAC, this supply is filtered via a line filter to attenuate any electromagnetic interference between the drive and line. The line filter feeds a line reactor which protects the AC Drive from any transient surges. The magnetic field of the reactor also limits the current rise rate reducing nuisance tripping and harmonics.

The smart line module is coupled to a Sinamics S120 single motor module (MOMO) (6SL3120-1TE21-0AD0), providing the MOMO with control voltage and DC Link voltage for the motor, a communications cable is connected between the MOMO and control unit for control and feedback. The MOMO output is connected to a motor inductor to smooth out current fluctuations caused by the power-switching electronics by adding extra inductance, the AC motor is connected to the opposite side of the inductors. The AC motor also has an incremental encoder connected to a Sinamics sensor module which converts the angular motion of the motor into a speed or direction signal that can be read by the PLC.

The test rig safety is monitored via a fail-safe input card which monitors signals from safety equipment such as emergency-stops, guard door switches and two push-buttons “Start” and “Stop”. These safety signals are constantly monitored to ensure all safety functions are in their correct state to allow for machine operation. A logic is written by the software engineer, this determines the conditions that the safety inputs must be in to allow the safety outputs to energise. These safety outputs control the DCM drive enable, S120 AC drive enable, DC motor fan and door guard switch solenoid. Therefore, the motors are only able to run when all safety conditions are met and the door cannot be unlocked until it is safe to do so as determined by the PLC.

All components have suitable overcurrent protection in the form of MCBs for the AC components and fuses for DC components. The control panel can only be opened when the mechanically interlocked main isolator is off in turn disconnecting the supply power to the machine.

A Picoscope oscilloscope is used for measuring key motor parameters during operation, four probes are connected within this practical reading Line Voltage, Phase Current, Armature Voltage and Armature Current. The waveforms of the motor are monitored using Picoscope 6 where accurate measurements are made. A Chauvin-Arnoux Power & Quality Analyser is connected to the line side of the DCM, measuring three-phase current this instrument provides readings for power values including Wattage (W), Volt-Amps Reactive (VAR), Volt-Amps (VA) and Power Factor (PF)

Figures 33-38 shows the basic overview electrical schematics of the control system.

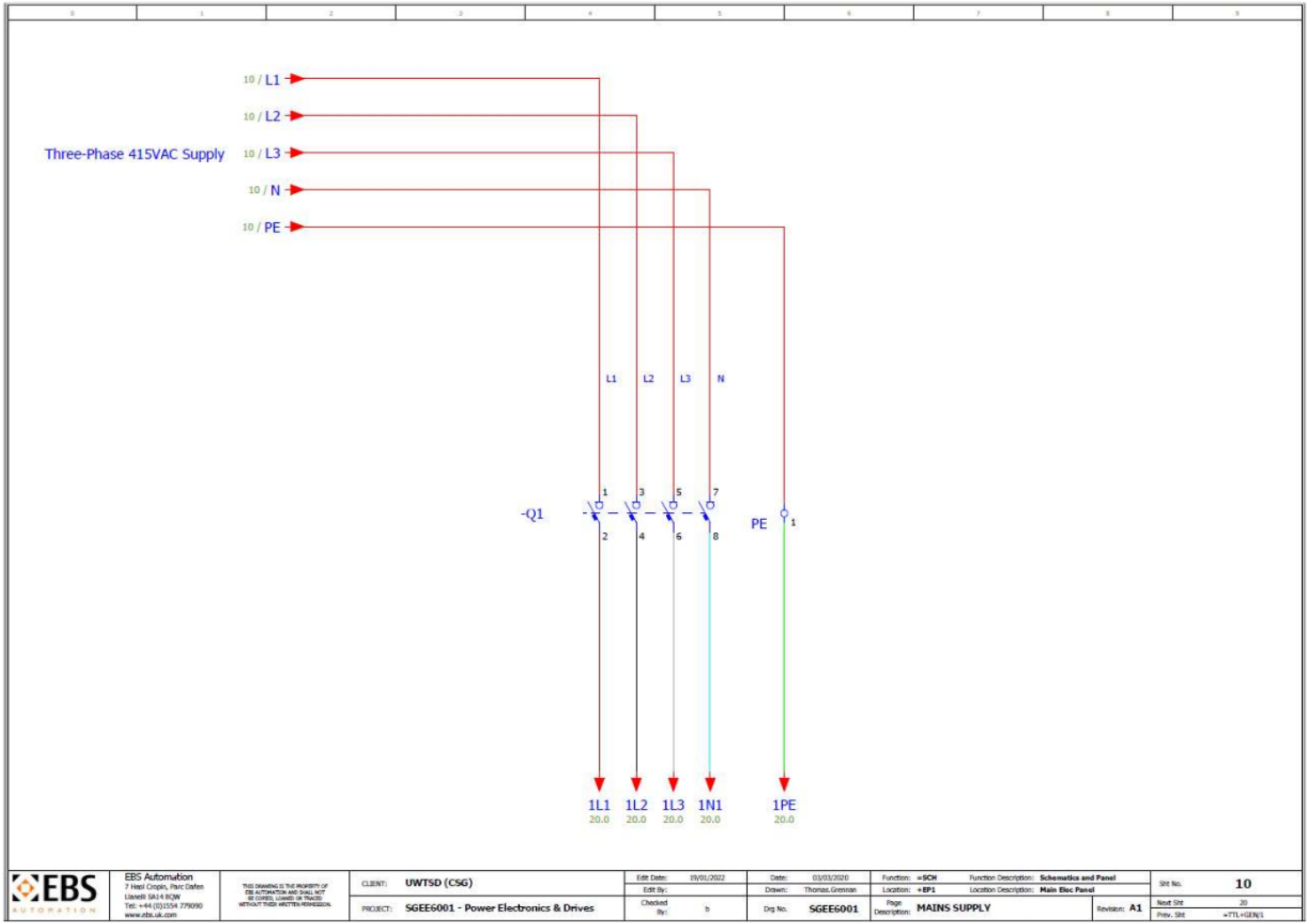


Figure 33 – Practical Control Panel Schematics: Mains Supply

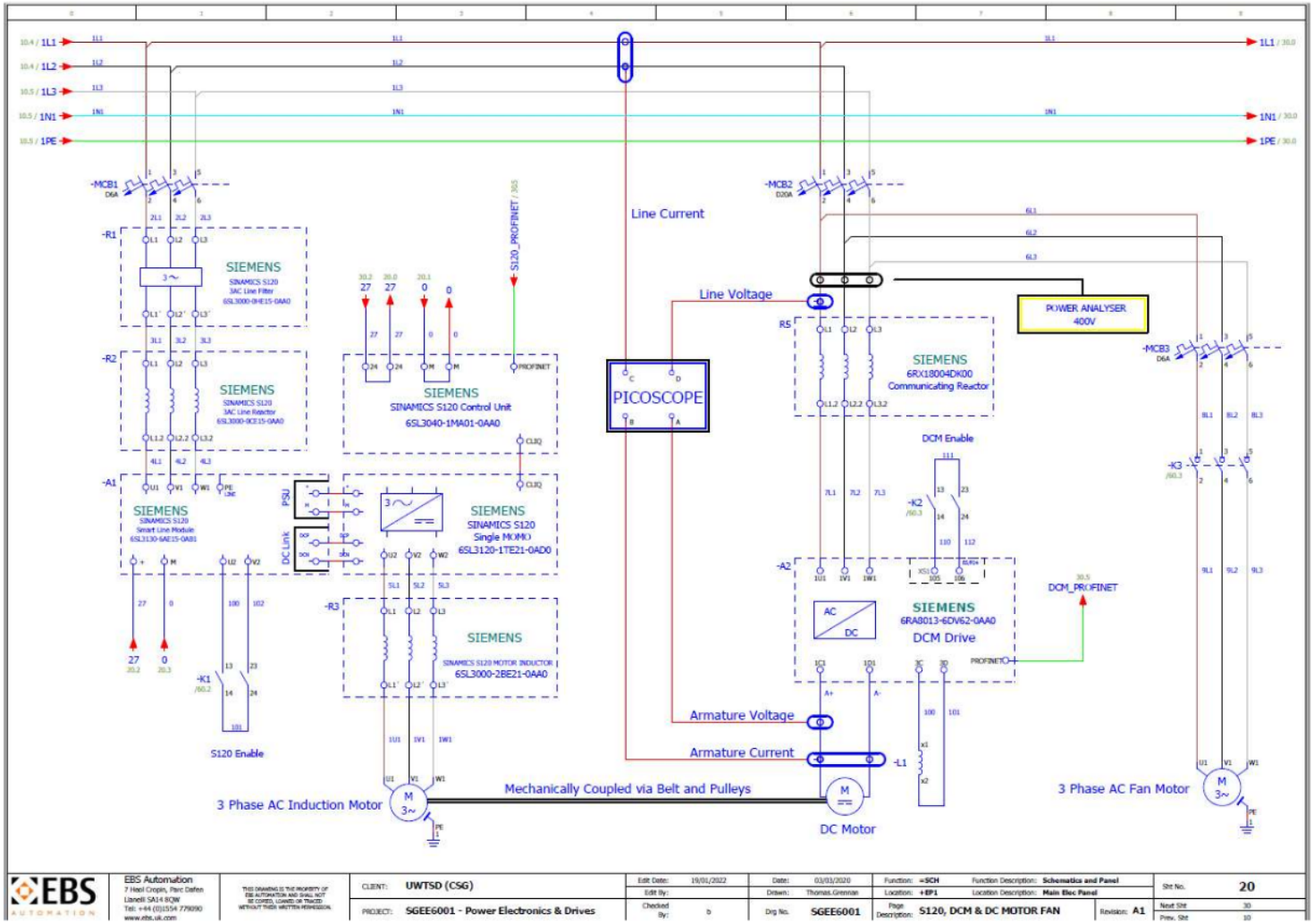


Figure 34 Practical Control Panel Schematics: S120, DCM & DC Motor (Inc. Picoscope & Power Analyser)

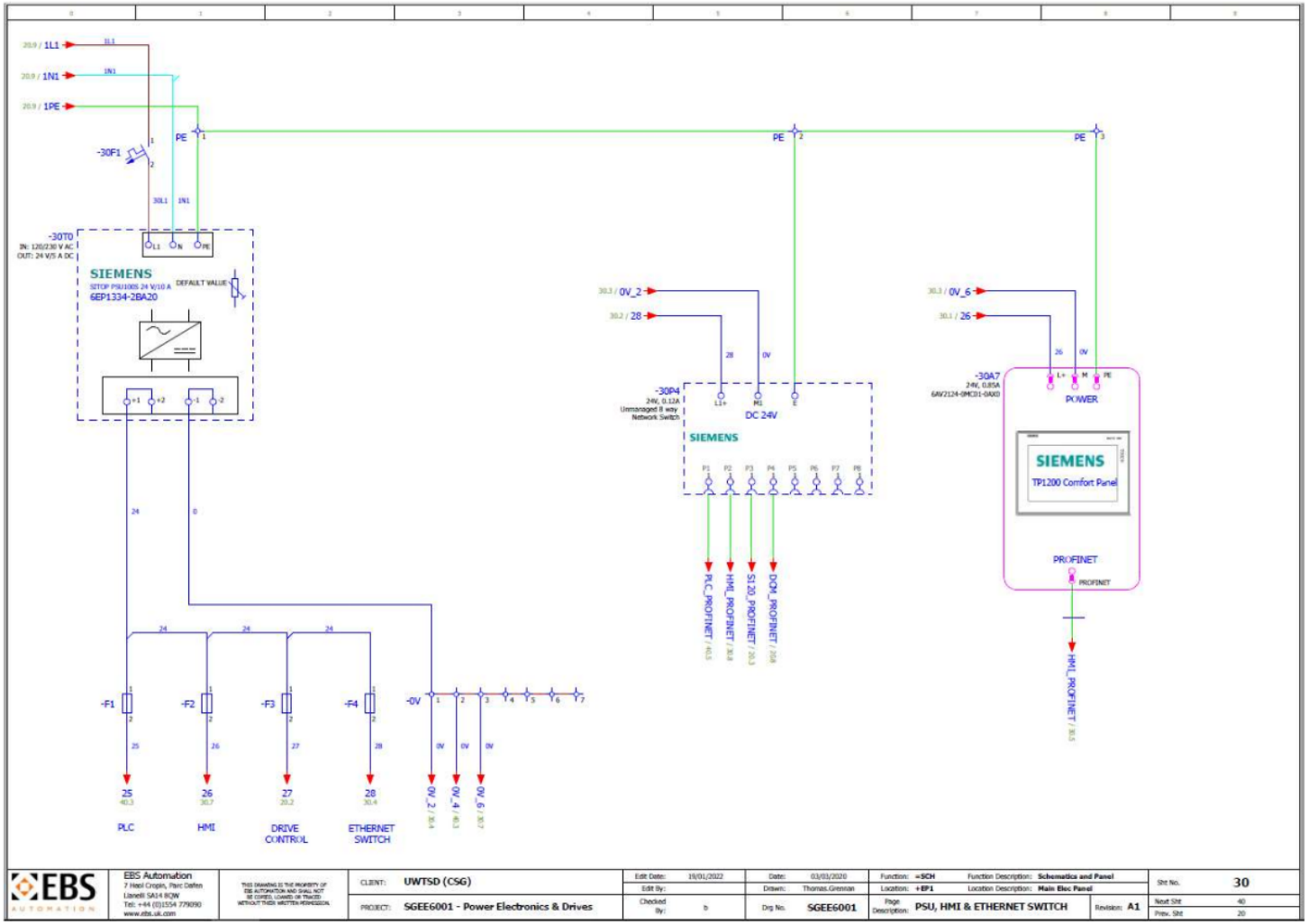


Figure 35 - Practical Control Panel Schematics: 24V Distribution, HMI and Ethernet Switch

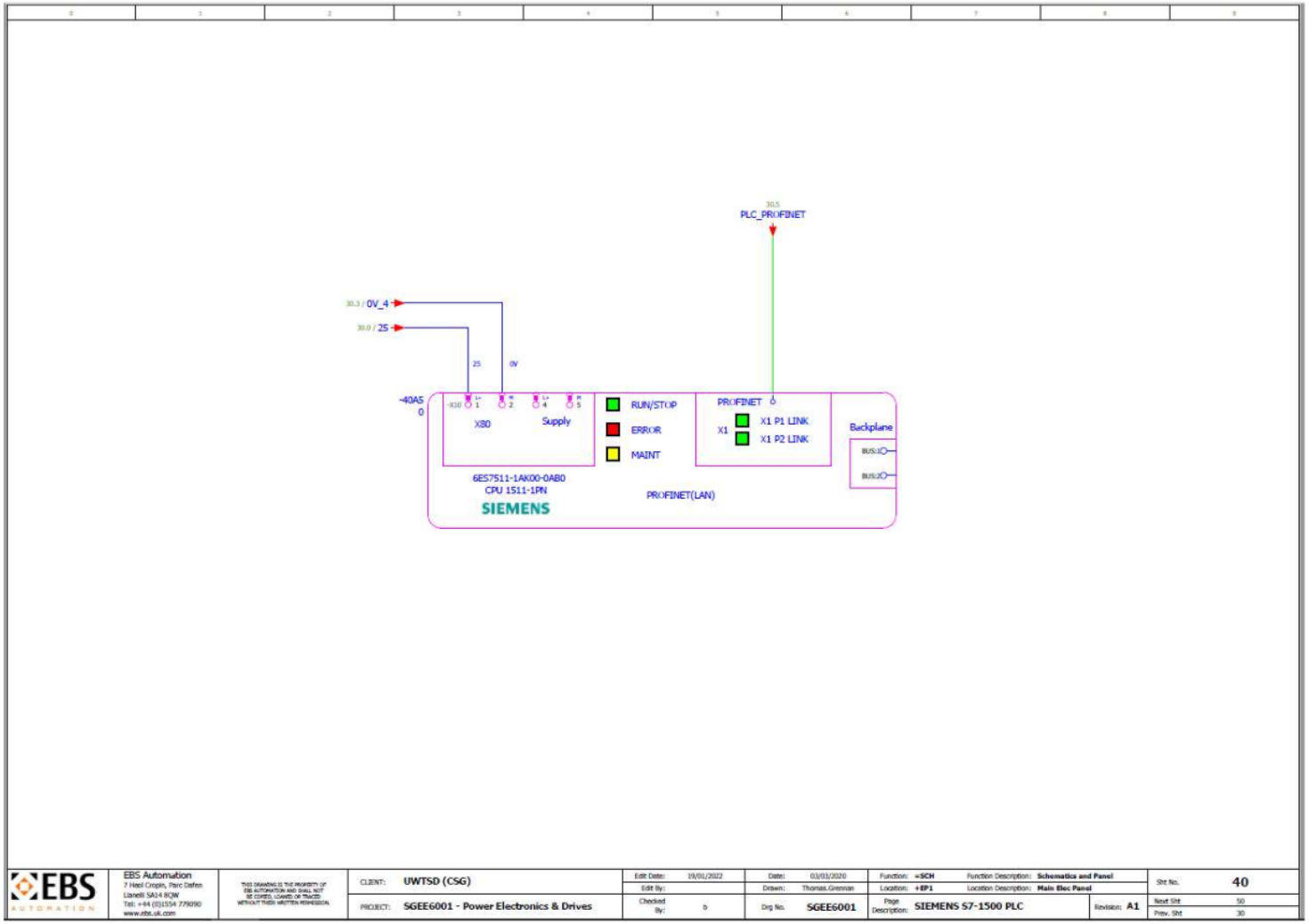


Figure 36 – Practical Control Panel Schematics: Siemens S7-1500 PLC

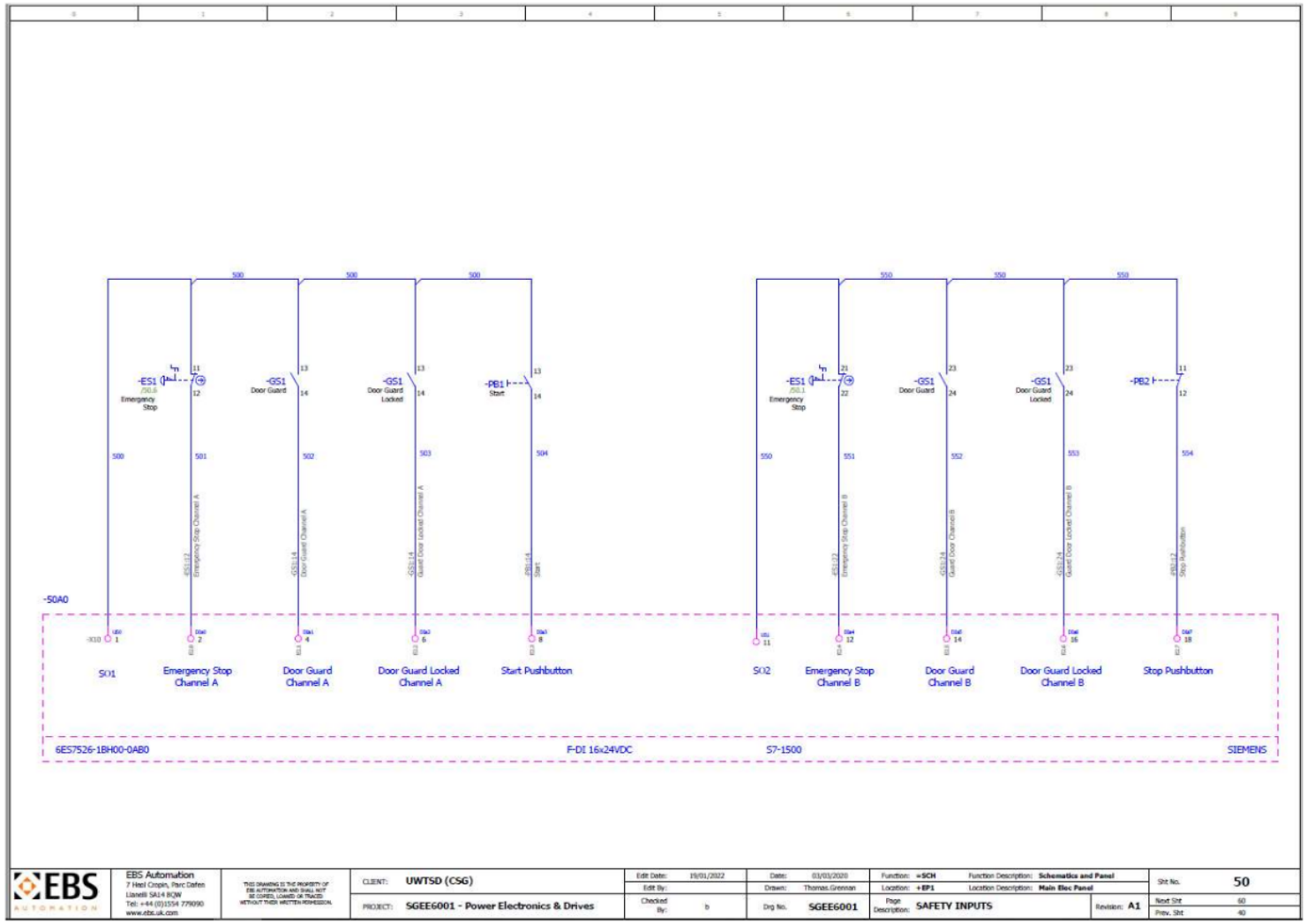


Figure 37 – Practical Control Panel Schematics: Safety Inputs

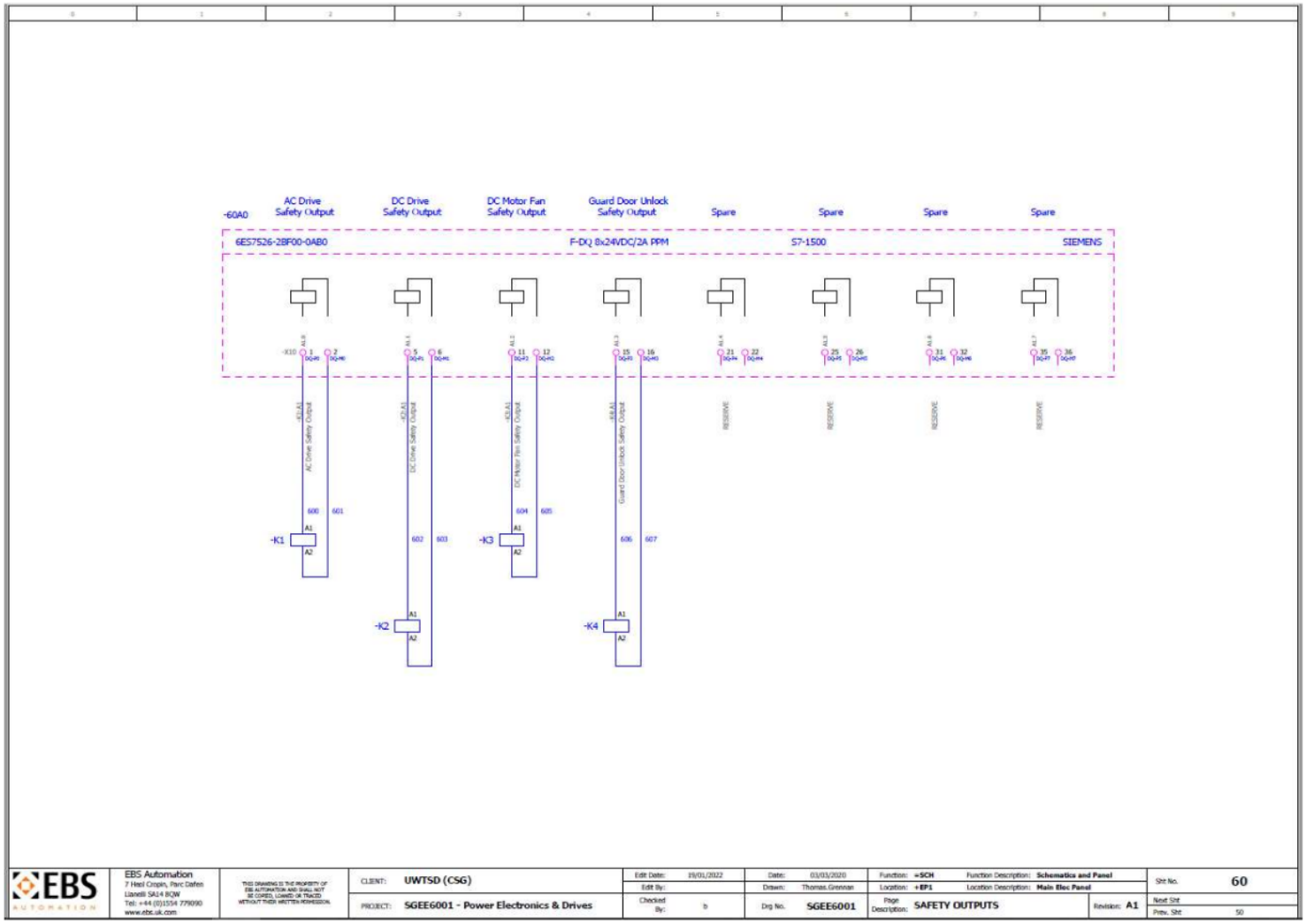


Figure 38 - Practical Control Panel Schematics: Safety Outputs

7.3.2 Demonstration of Four Quadrant Operation

Figure 39 shows the Picoscope graphs of the DC motor operating in quadrant 1. Both armature voltage and armature current are positive, indicating that the DC motor is forward motoring.

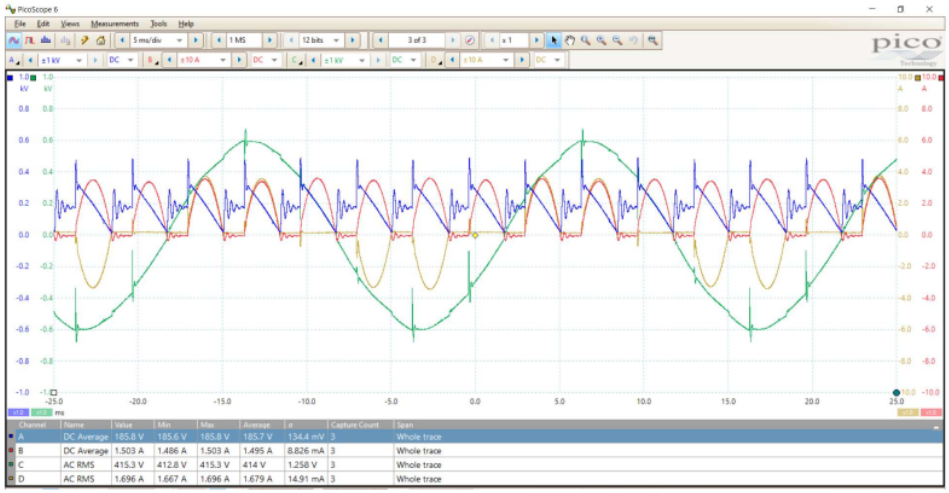


Figure 39 – Practical: Quadrant 1 operation (Picoscope)

Figure 40 displays the HMI during the first quadrant operation, the trace graph shows that both speed and torque are positive. Data written to the PLC from the DCM enables further judgment to be made, the firing angle is below 90˚, both armature current and voltage are positive, with the back EMF being a lower magnitude than the armature voltage. It is determined that quadrant 1 is forward motoring, with the DCM operating in bridge 1.

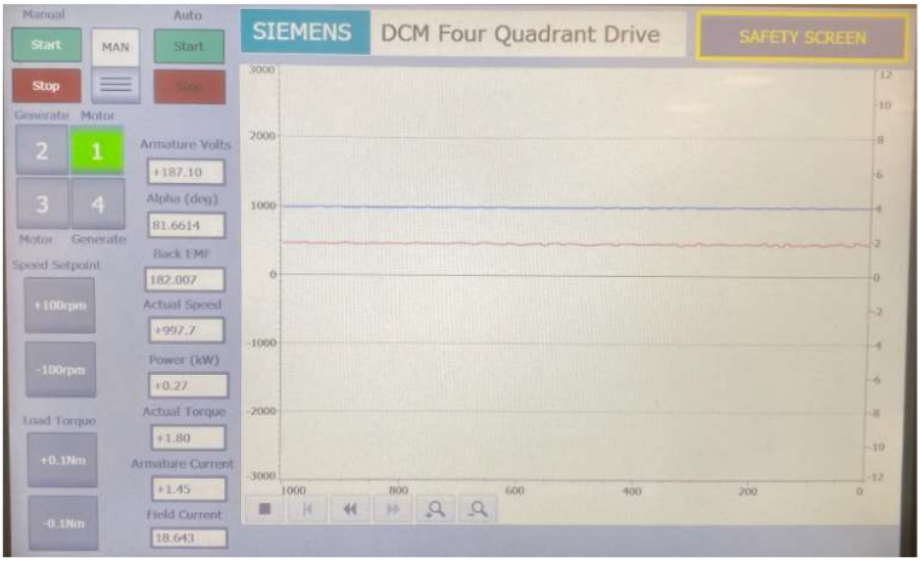


Figure 40 - Practical: Quadrant 1 operation (HMI)

Figure 41 shows the Picoscope graphs of the DC motor operating in quadrant 2. Armature voltage is positive; however, armature current is now negative indicating that the DC motor is forward braking.

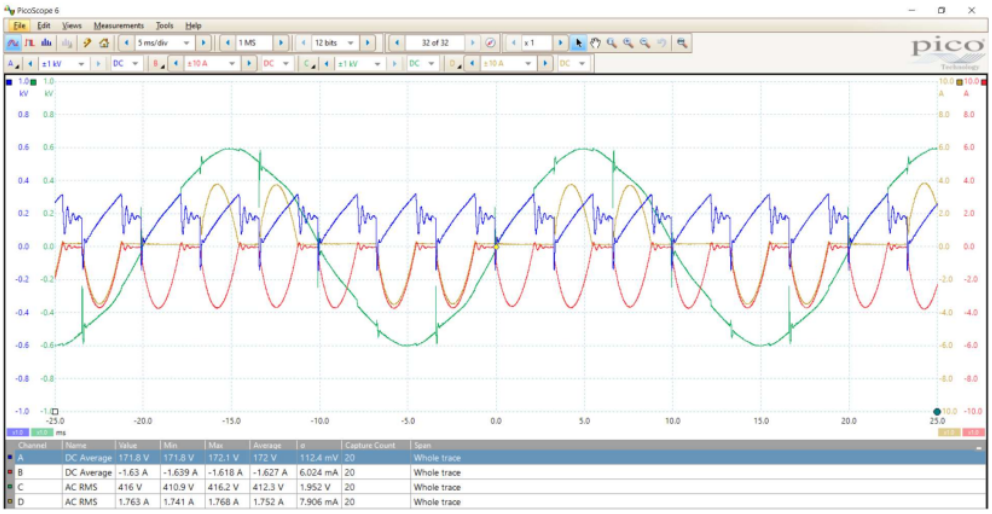


Figure 41 Practical: Quadrant 2 operation (Picoscope)

Figure 42 displays the HMI during the second quadrant operation, the trace graph shows that speed is positive and torque is negative. From the data written to the PLC from the DCM it is seen that the firing angle is greater than 90˚, armature current is negative and armature voltage is positive, with the back EMF being a greater magnitude than the armature voltage. It is determined that quadrant 2 is forward braking, with the DCM operating in bridge 2.

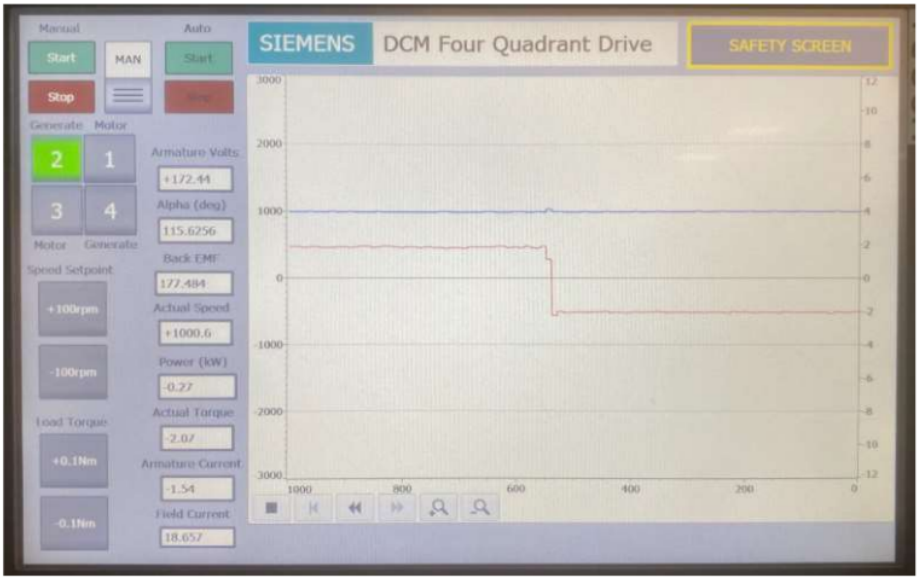


Figure 42 Practical: Quadrant 2 operation (HMI)

Figure 43 shows the Picoscope graphs of the DC motor operating in quadrant 3. Both armature voltage and armature current are negative. Quadrant 3 is almost identical to quadrant 1, with the exception of armature voltage and current being flipped across the X axis.

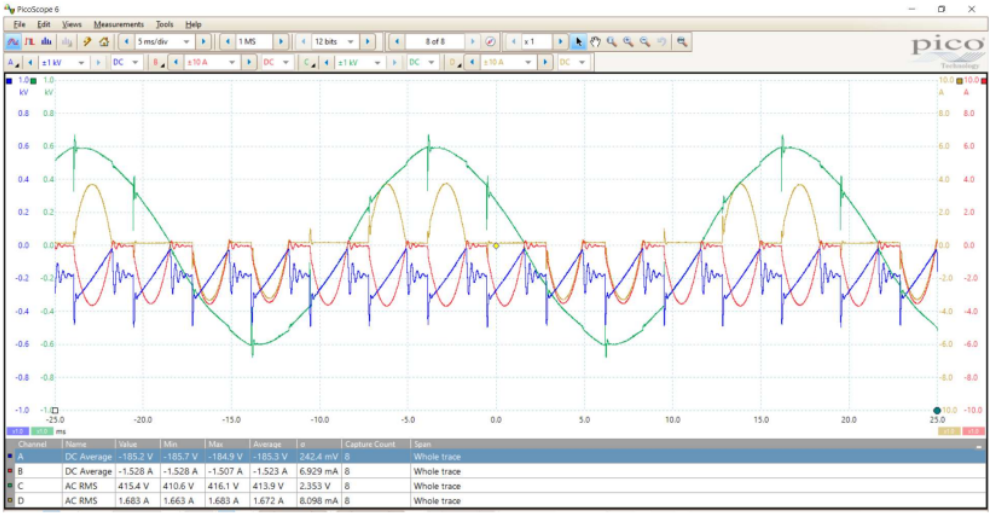


Figure 43 - Practical: Quadrant 3 operation (Picoscope)

Figure 44 displays the HMI during the third quadrant operation, the trace graph shows both speed and torque are negative, a mirror image of quadrant 1. The HMI shows it has a firing angle less than 90˚, both armature current and voltage are negative. The armature voltage is a greater magnitude than the back EMF. It is determined that quadrant 3 is reverse motoring, with the DCM operating in bridge 2.

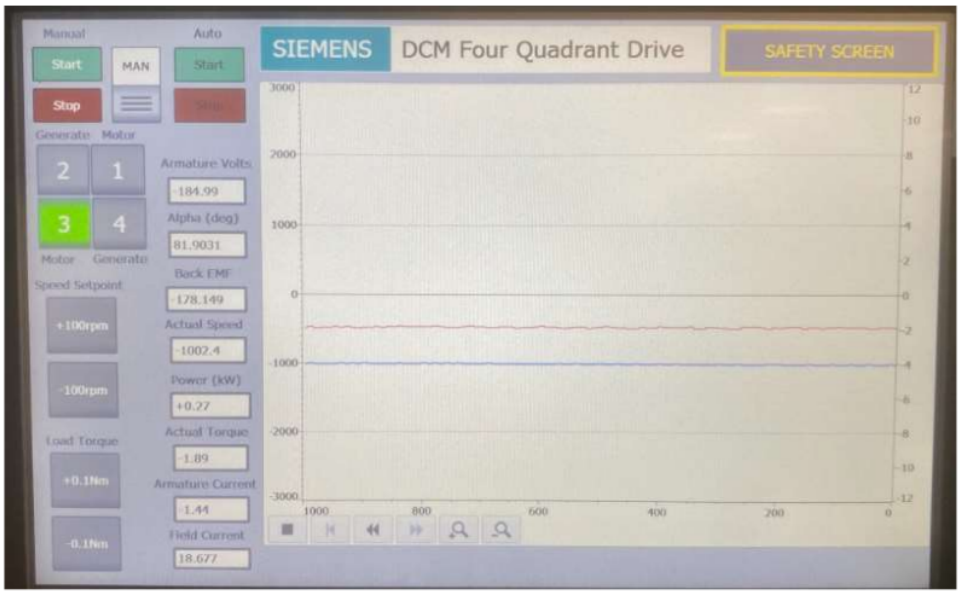


Figure 44 - Practical: Quadrant 3 operation (HMI)

Figure 45 shows the Picoscope graphs of the DC motor operating in quadrant 4. Armature voltage is negative; however, armature current is positive.

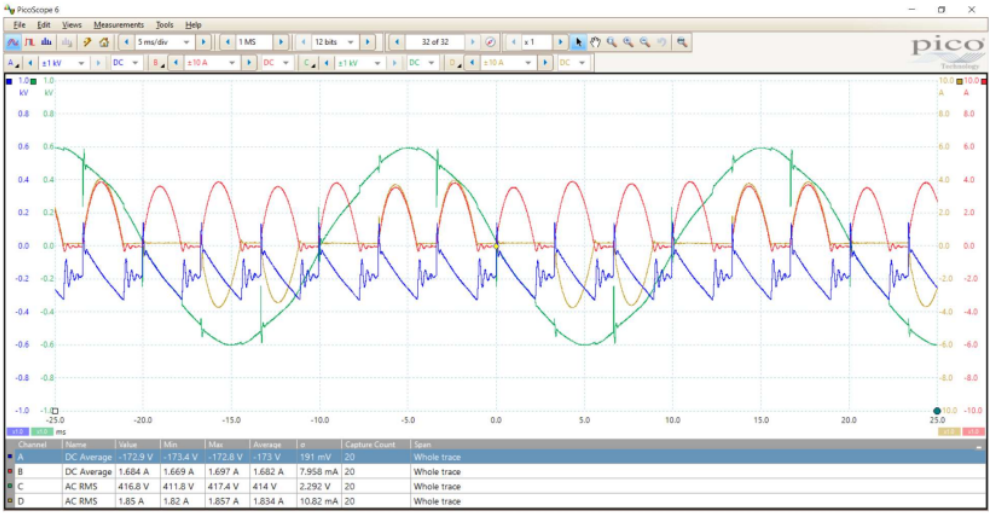


Figure 45 - Practical: Quadrant 4 operation (Picoscope)

Figure 46 displays the HMI during the fourth quadrant operation, the trace graph shows that torque is positive and speed is negative. The firing angle is greater than 90˚, armature current is positive and armature voltage is negative, with the back EMF being a greater magnitude than the armature voltage. It is determined that quadrant 4 is reverse braking, with the DCM operating in bridge 1.

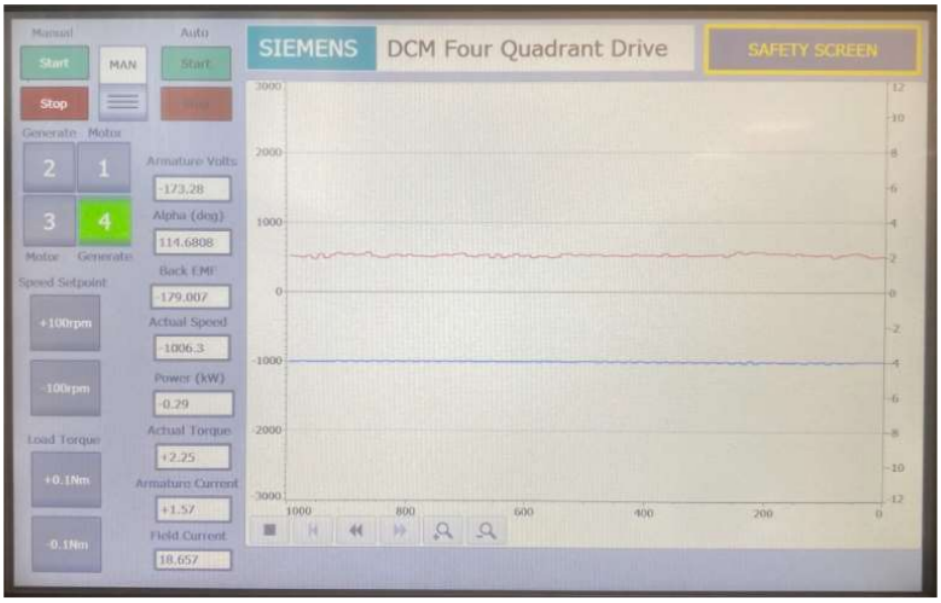
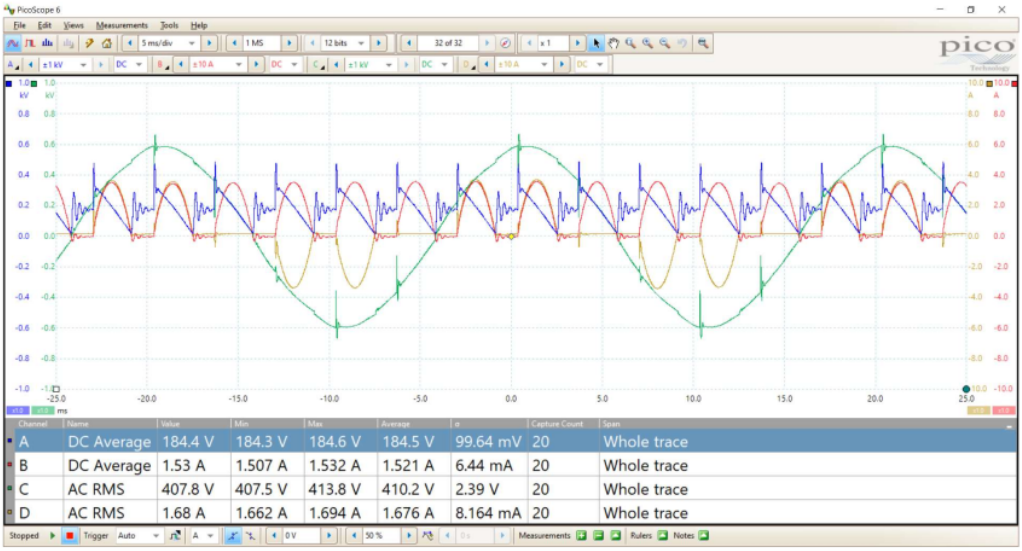


Figure 46 - Practical: Quadrant 4 operation (HMI)

7.3.3 3 values of speed at a constant torque

The DC drive is run in quadrant 1 where it is motoring in its forward direction whilst displaying discontinuous current. The speed set-point is altered for three different values of speed to determine the effect the motors parameters. Three set-points are chosen at around 1000rpm, 1500rpm and 2000rpm.

Set-Point 1 – 1000 RPM



Channel	Name	Value	Min	Max	Average	σ	Capture Count	Span
A	DC Average	184.4 V	184.3 V	184.6 V	184.5 V	99.64 mV	20	Whole trace
B	DC Average	1.53 A	1.507 A	1.532 A	1.521 A	6.44 mA	20	Whole trace
C	AC RMS	407.8 V	407.5 V	413.8 V	410.2 V	2.39 V	20	Whole trace
D	AC RMS	1.68 A	1.662 A	1.694 A	1.676 A	8.164 mA	20	Whole trace

Figure 47 – Practical Speed test: Setpoint 1 Picoscope

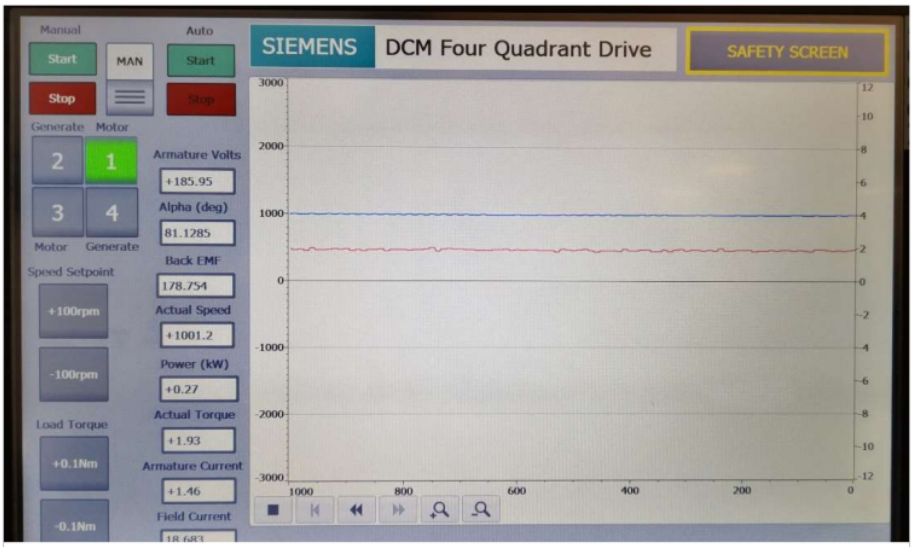


Figure 48 - Practical Speed test: Setpoint 1 HMI

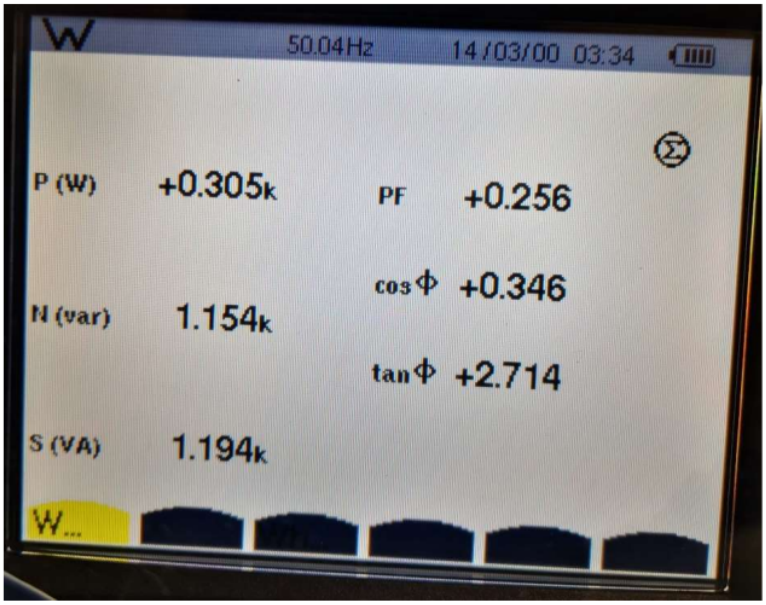


Figure 49 - Speed test: Setpoint 1 Power Analyser

Set-Point 2 – 1500RPM

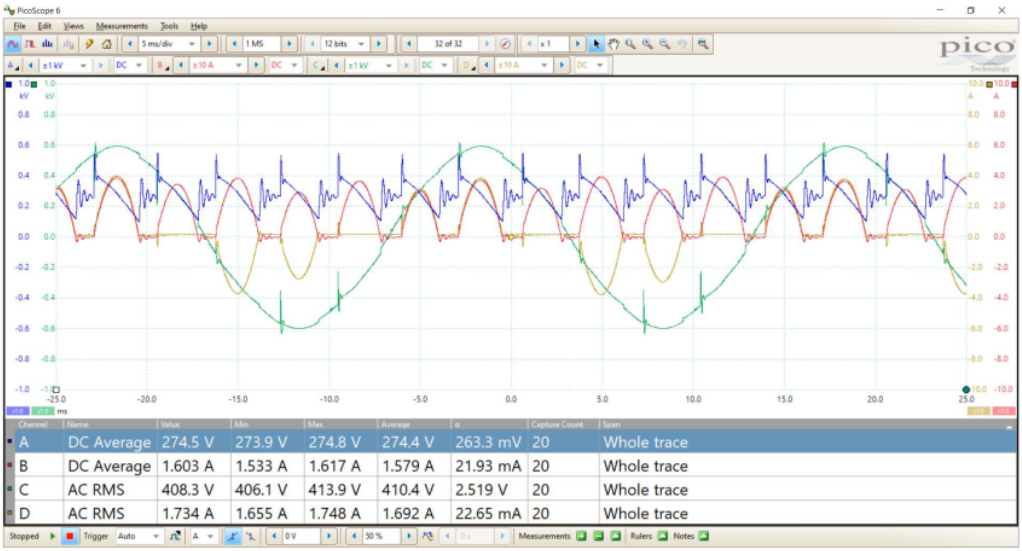


Figure 50 - Practical Speed test: Setpoint 2 Picoscope

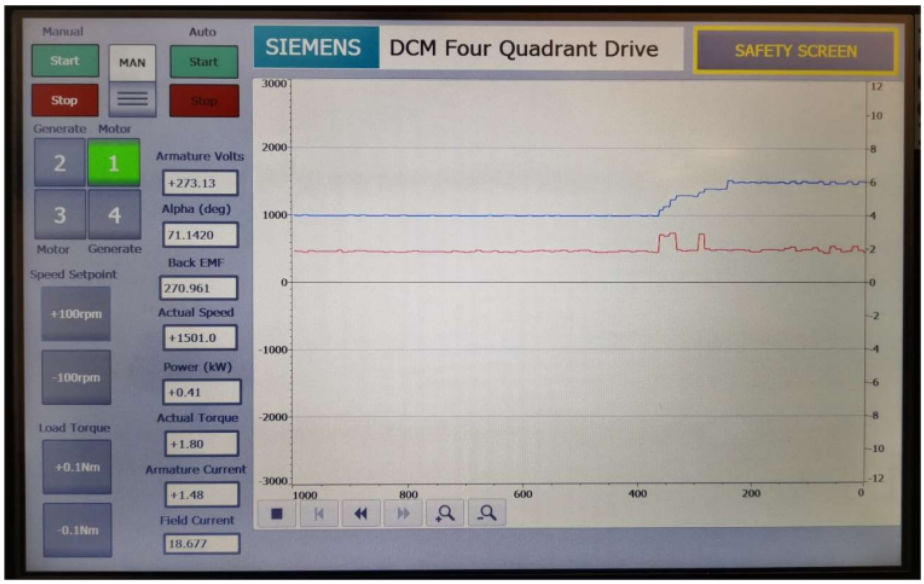


Figure 51 - Practical Speed test: Setpoint 2 HMI

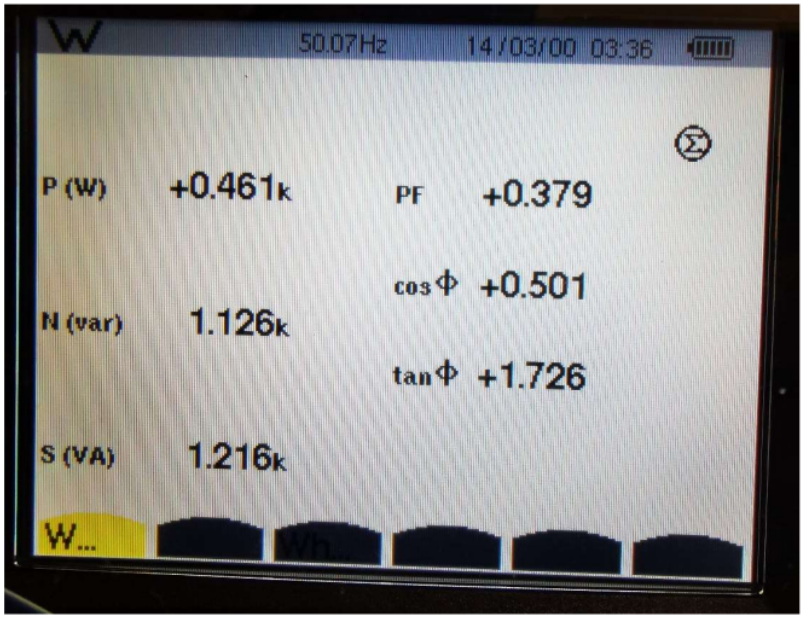


Figure 52 - Practical Speed test: Setpoint 2 Power Analyser

Set-Point 3 – 2000PM

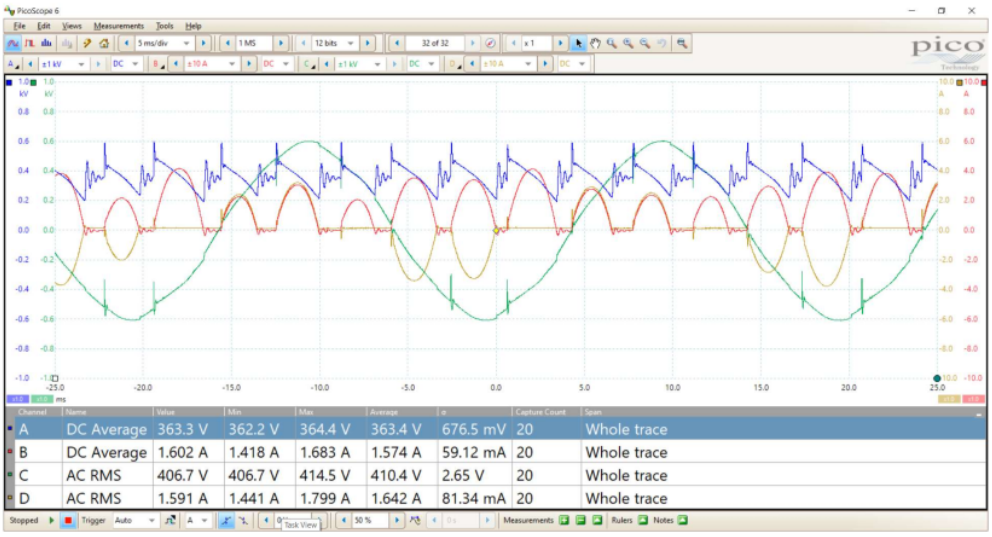


Figure 53 - Practical Speed test: Setpoint 3 Picoscope

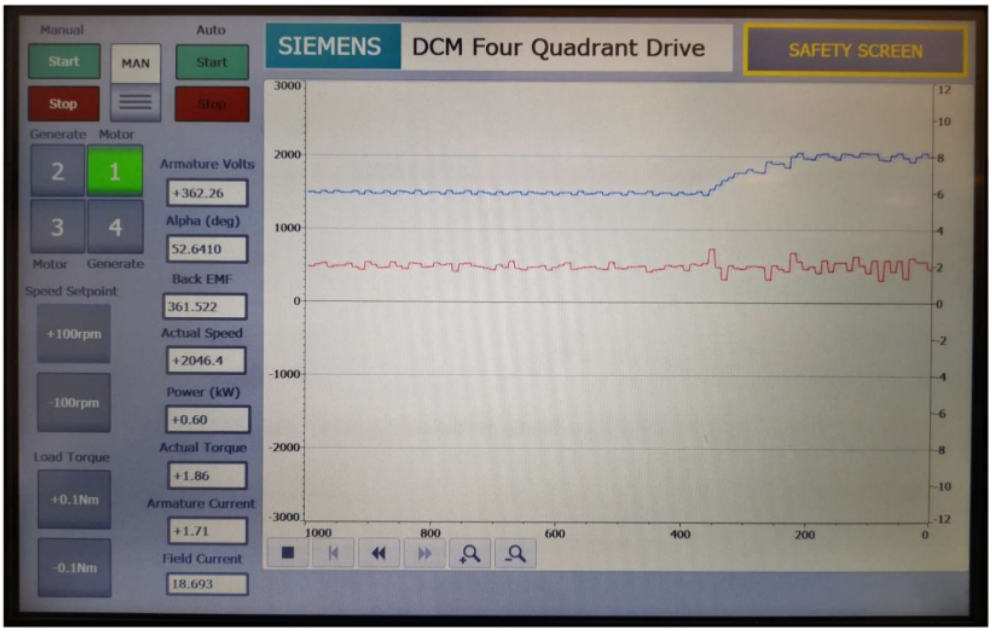


Figure 54 - Practical Speed test: Setpoint 3 HMI

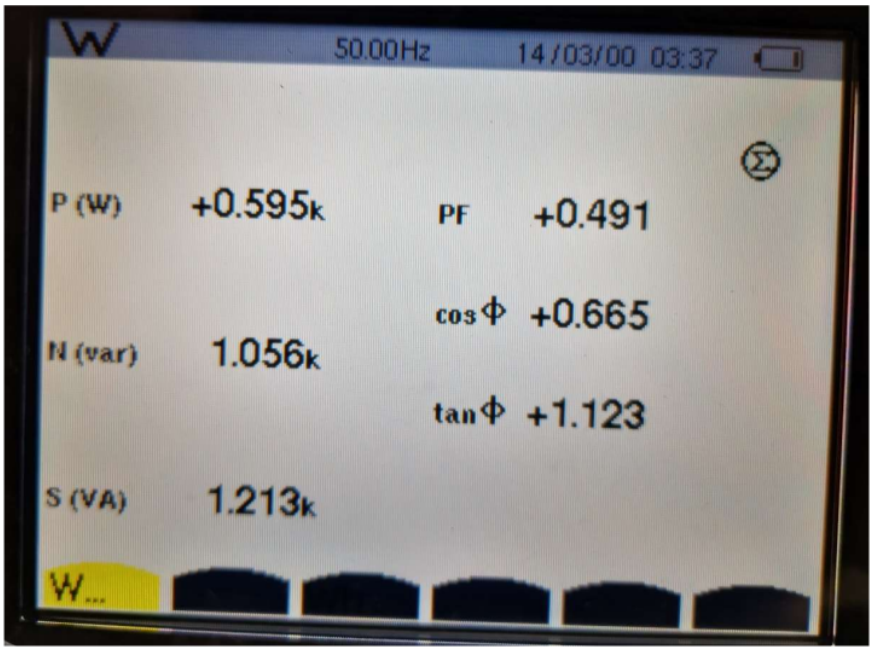


Figure 55 - Practical Speed test: Setpoint 3 Power Analyser

Mean voltage calculation for set-point 1

Using values obtained from figures 46 and 47 the average armature voltage is calculated from the Picoscope waveform and the DCMs parameters that have been written to the PLC.

Area A:

$$Area\ A = E\ x\ \gamma\ =\ E\left(\alpha - \frac{\pi}{3}\right)$$

Area B:

$$Area\ B = Vmax \int_{\frac{\pi}{3}+\alpha}^{\pi} \sin(\theta) d\theta\ = Vmax[-cos\theta]\ \begin{matrix}\pi \\ \frac{\pi}{3}+\alpha\end{matrix}$$

∴

$$Area\ B\ =\ Vmax\left[-cos\pi - -\cos\left(\frac{\pi}{3}+\alpha\right)\right]\ =\ Vmax\left[1+\frac{1}{2}cos\alpha - \frac{\sqrt{3}}{2}sin\alpha\right]$$

V_{mean}:

$$Vmean = \frac{Area\ A + Area\ B}{\frac{\pi}{3}}$$

Set-Point 1, HMI Armature Voltage – 185.95V:

$$E = 178.754V$$
$$\propto = 81.1285^{\circ}$$
$$V_{Max} = 589.6V$$

Where $\propto$ is converted into radians:

$$\propto = 81.125 \times \frac{\pi}{180} = 1.416$$

Area A:

$$Area\ A = E\left(\alpha - \frac{\pi}{3}\right) = 178.754(1.416 - 1.0472) = 65.925V$$

Area B:

$$Area\ B = 589.6V\left[1 + \frac{1}{2}cos(1.416) - \frac{\sqrt{3}}{2}sin(1.416)\right] = 130.592V$$

V_{Mean}:

$$Vmean = \frac{65.925 + 130.592}{\frac{\pi}{3}} = 187.6599V$$

7.3.4 3 values of torque at a constant speed

The DC drive is run in quadrant 1 where it is motoring in its forward direction whilst displaying continuous current. The torque set-point is altered for three different values to determine the effect this has on motors parameters at fixed speed. Three set-points are chosen at around 6.12Nm, 4.70Nm and 3.60Nm.

Torque Set-Point 1 – 6.12Nm

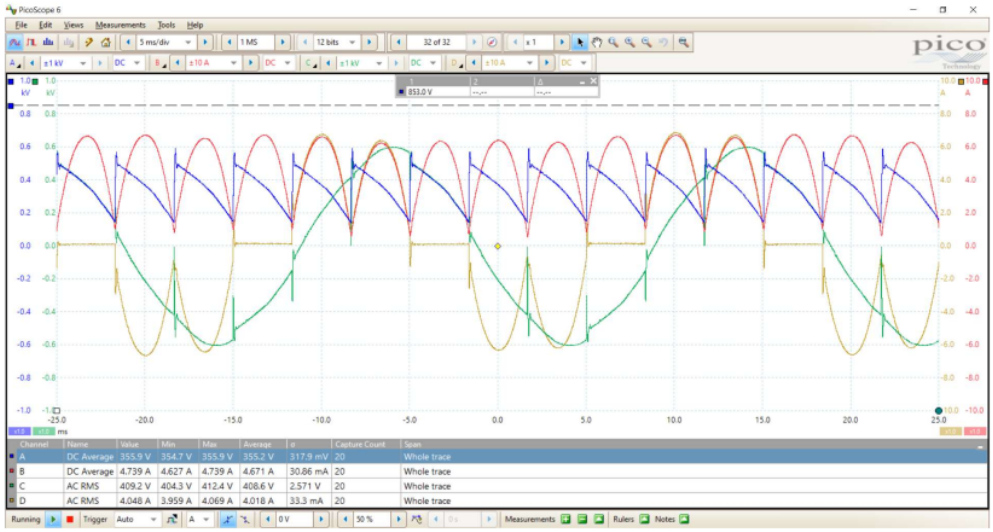


Figure 56 - Practical Torque test: Setpoint 1 Picoscope

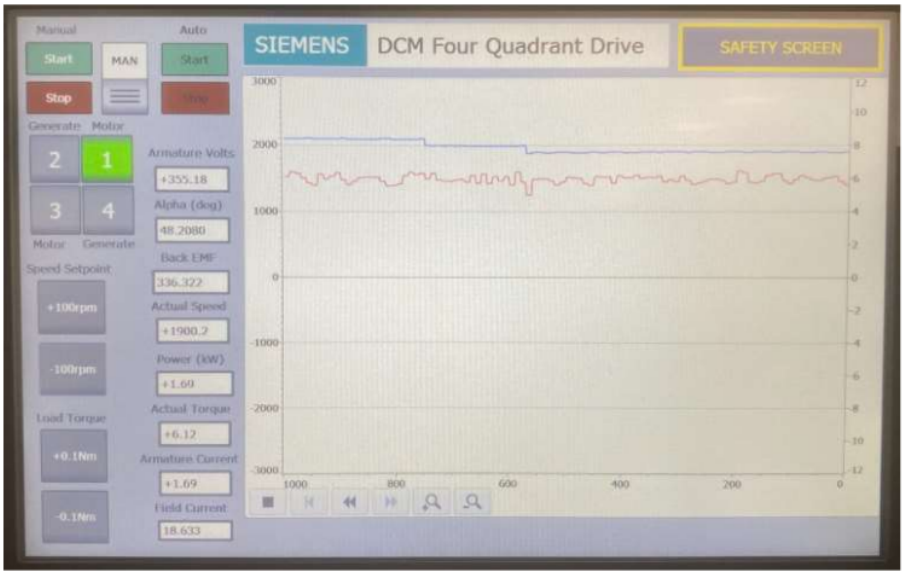


Figure 57 - Practical Torque test: Setpoint 1 HMI

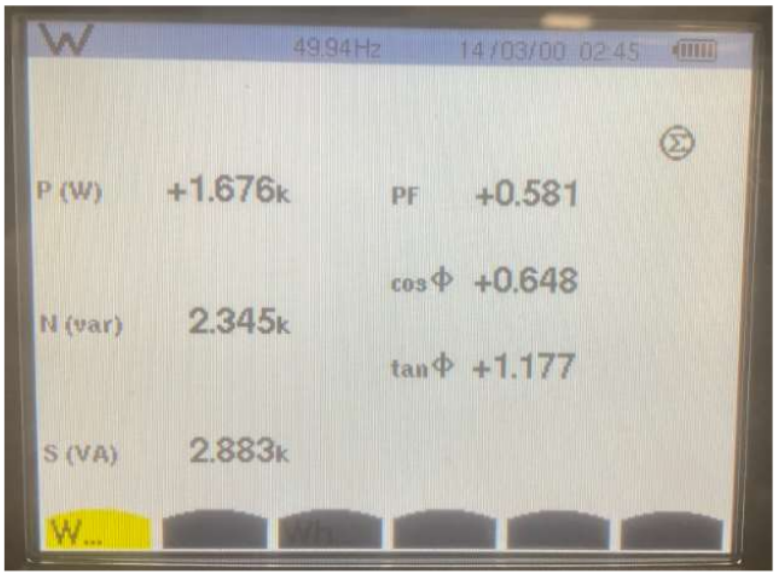


Figure 58 - Practical Torque test: Setpoint 1 Power Analyser

Torque Set-Point 2 – 4.70Nm

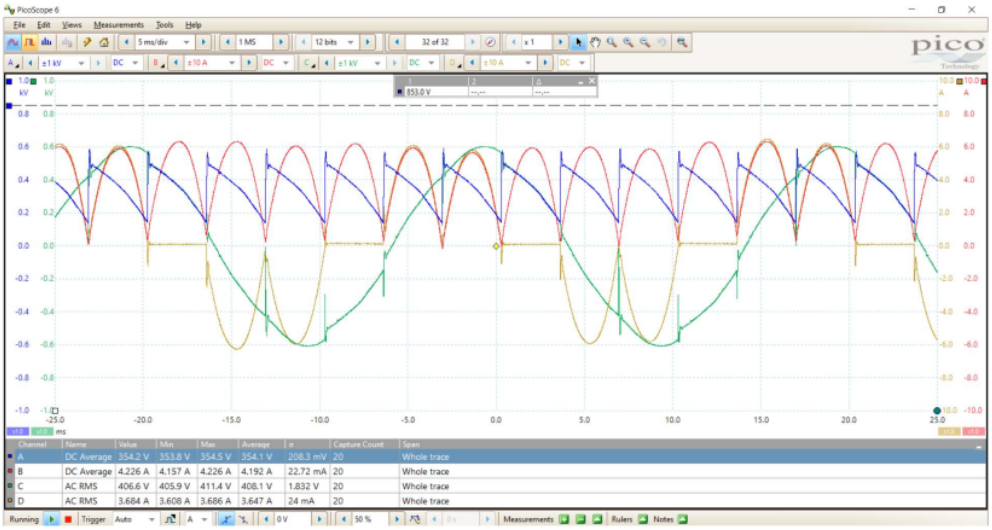


Figure 59 - Practical Torque test: Setpoint 2 Picoscope

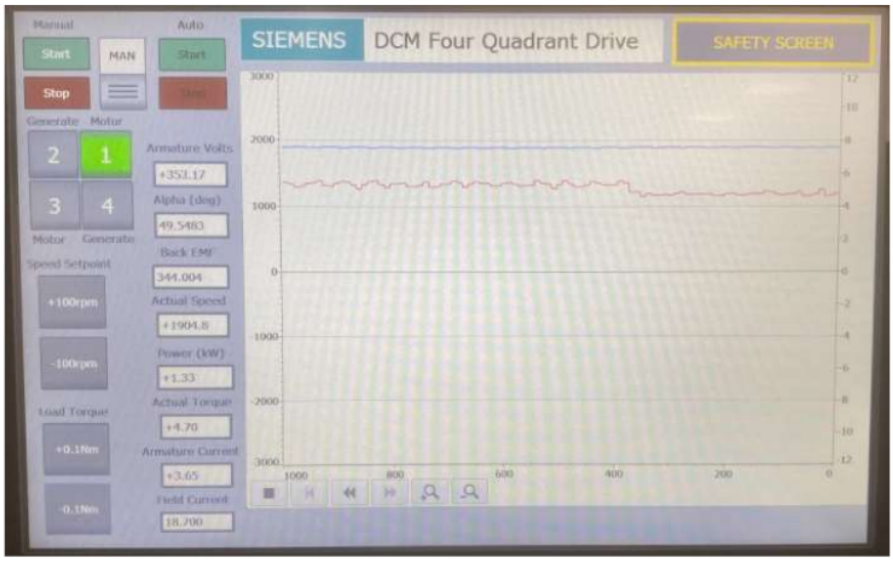


Figure 60 - Practical Torque test: Setpoint 2 HMI

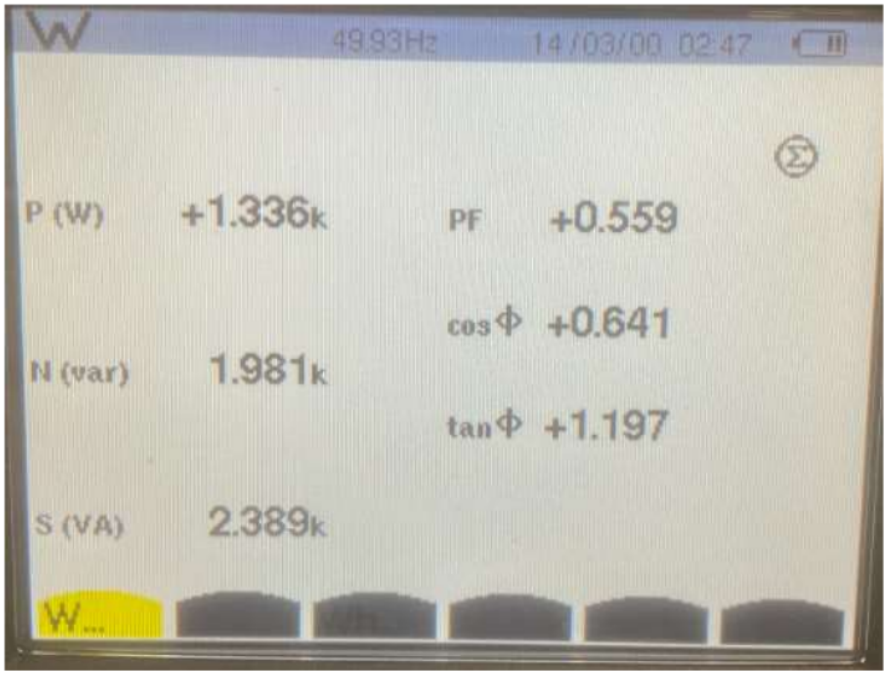


Figure 61 -Practical Torque test: Setpoint 2 Power Analyser

Torque Set-Point 3 – 3.60Nm

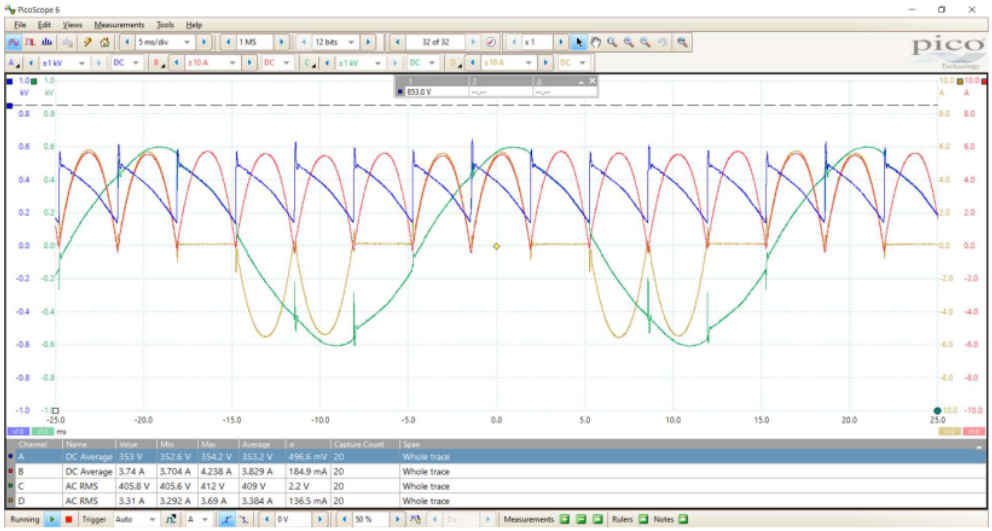


Figure 62 - Practical Torque test: Setpoint 3 Picoscope

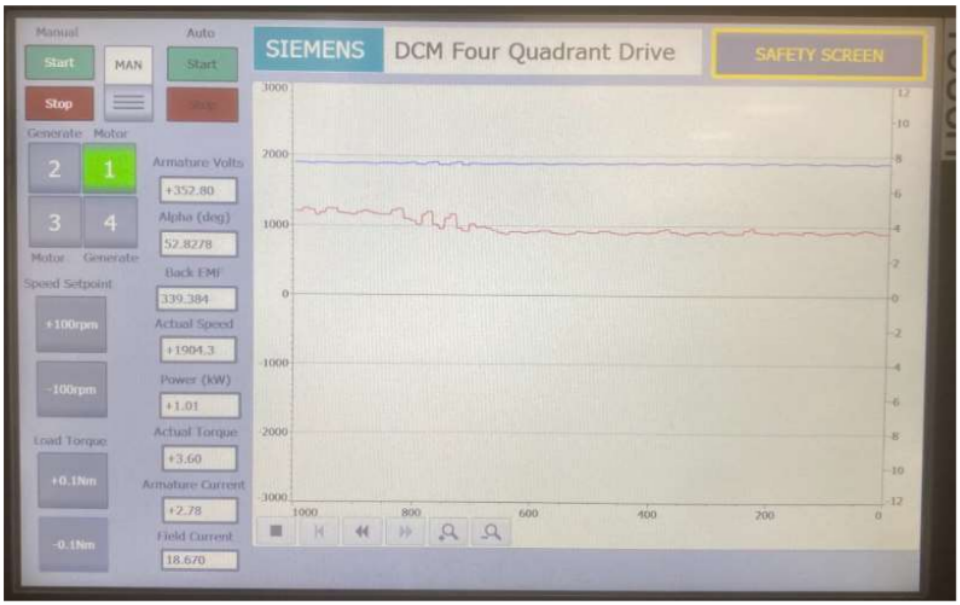


Figure 63 - Practical Torque test: Setpoint 3 HMI

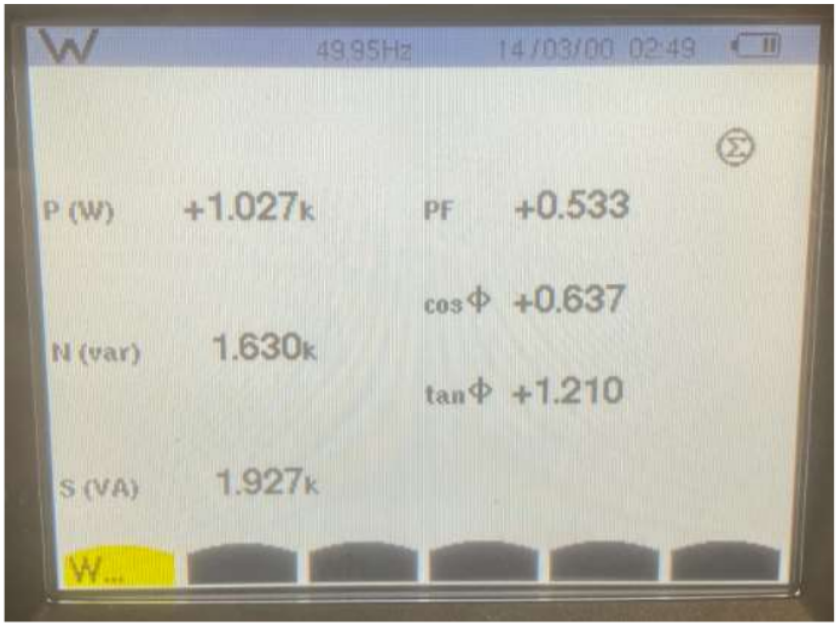


Figure 64 - Practical Torque test: Setpoint 3 Power Analyser

1809799

GRADEMARK REPORT

FINAL GRADE

85/100

GENERAL COMMENTS

Instructor

PAGE 1

Text Comment. Word count exceeded

Text Comment. Good summary but it is too long

Text Comment. Excellent evidence of research, all relevant but again too long and too much detail

Text Comment. Your assessment of business and customer needs is particularly good

Text Comment. Simulation, design adaptation and practical work are excellent with support for results from research

Text Comment. Good conclusions and recommendation presented

Text Comment. However, report is too long

PAGE 2

PAGE 3

PAGE 4

PAGE 5

PAGE 6

PAGE 7

PAGE 8

PAGE 9

PAGE 10

PAGE 11

PAGE 12

PAGE 13

PAGE 14

PAGE 15

PAGE 16

PAGE 17

PAGE 18

PAGE 19

PAGE 20

PAGE 21

PAGE 22

PAGE 23

PAGE 24

PAGE 25

PAGE 26

PAGE 27

PAGE 28

PAGE 29

PAGE 30

PAGE 31

PAGE 32

PAGE 33

PAGE 34

PAGE 35

PAGE 36

PAGE 37

PAGE 38

PAGE 39

PAGE 40

PAGE 41

PAGE 42

PAGE 43

PAGE 44

PAGE 45

PAGE 46

PAGE 47

PAGE 48

PAGE 49

PAGE 50

PAGE 51

PAGE 52

PAGE 53

PAGE 54

PAGE 55

PAGE 56

PAGE 57

PAGE 58

PAGE 59

PAGE 60
PAGE 61
PAGE 62
PAGE 63
PAGE 64
PAGE 65
PAGE 66
PAGE 67
PAGE 68
PAGE 69
PAGE 70
PAGE 71
PAGE 72
PAGE 73

GRADING FORM: NEW CSG-RUBRIC

THOMAS GRENNAN	**85**

1. ENGAGEMENT WITH LITERATURE

Exceptional engagement with an extensive range of relevant and credible literature, informed by the latest research. High-level referencing skills consistently and professionally applied. (18/20)	**18**

2. KNOWLEDGE AND UNDERSTANDING



Exceptionally coherent and detailed knowledge and systematic understanding of the principles and theories of the subject, well-informed by current research and scholarship. A critical, sophisticated and nuanced awareness of the ambiguities and limitations of knowledge. (17/20)

17

3. COGNITIVE AND INTELLECTUAL



Exceptional critical thinking, analysis, synthesis and evaluation based on judiciously selected evidence. Ability to investigate contradictory or incomplete information and make strong, persuasive, arguments and sophisticated, nuanced, judgements. Evidence of independent thought and ability to 'see beyond the question', suggesting an outstanding grasp of the broader field and wider concepts. (18/20)

18

4. PRACTICAL APPLICATION



Exceptional levels of application and deployment skills in unpredictable, practical contexts, drawing skilfully on the latest research within the discipline. Can identify complex problems and propose sophisticated solutions. Assimilation and development of cutting edge processes and techniques. (18/20)

18

5. TRANSFERABLE SKILLS



Can communicate professionally confidently and consistently in a suitable format. Work is coherent, very fluent and is presented professionally. Can work autonomously with initiative. Where relevant can work professionally within a team, showing leadership skills as appropriate, managing conflict and meeting obligations. Demonstrates excellent graduate employment skills and an appetite for further development. (14/20)

14